

DYNAMIC SIMULATION OF A 110 MW THERMAL  
UNIT AT PANKI THERMAL POWER STATION

By

MONY. N

ME

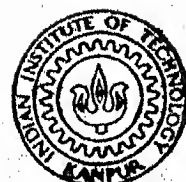
1979

M

MONY

DYN INDIAN INSTITUTE OF TECHNOLOGY, KANPUR

JUNE, 1979



DEPARTMENT OF MECHANICAL ENGINEERING

DYNAMIC SIMULATION OF A 110 MW THERMAL  
UNIT AT PANKI THERMAL POWER STATION

A Thesis Submitted  
In Partial Fulfilment of the Requirements  
for the Degree of  
**MASTER OF TECHNOLOGY**

By  
**MONY, N**

I.I.T. KANPUR  
CENTRAL LIBRARY  
**59255**  
Acc. No. **A**

23 AUG 1979

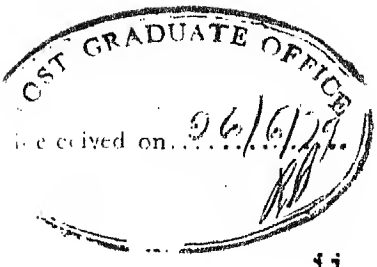
ME-1979-M-MONY-DYN

to the

**DEPARTMENT OF MECHANICAL ENGINEERING**

**INDIAN INSTITUTE OF TECHNOLOGY, KANPUR**

JUNE, 1979



ii

## CERTIFICATE

This is to certify that the work entitled DYNAMIC SIMULATION OF A 110 MW THERMAL UNIT AT PANKI THERMAL POWER STATION by Shri Mony. N. has been carried out under my supervision and has not been submitted elsewhere for the award of a degree.

Dr. B. Sahay  
Assistant Professor,  
Department of Mechanical Engg.  
Indian Institute of Technology  
Kanpur 208016, INDIA.

POST GRADUATE OFFICE  
This thesis has been approved  
for the award of the Degree of  
Master of Technology (M.Tech.)  
in accordance with the  
regulations of the Indian  
Institute of Technology Kanpur  
Dated. 4.7.79 4'

#### ACKNOWLEDGEMENT

I express my sincere gratitude to Dr. B. Sahay for his guidance throughout the period of this research.

I wish to thank Dr. P.V. Girijashankar for his keen interest in this problem and his fruitful and timely suggestions.

Thanks are also due to Mr. C.M. Abraham for his speedy typing of the manuscript.

Finally, I wish to thank my dear ones and sincere friends for extending their helping hands and encouragements throughout the course of study.

## SYNOPSIS

A 110 MW unit of the Panki Thermal Power Plant, Panki, is selected to develop a non-linear mathematical model. The model incorporates all the important components of the power plant and is systematically presented in the text. The entire system is divided into three subsystems for the convenience in the modelling. In the present integrated boiler-turbine model dynamics of forced draft fan, fuel feeding system and furnace are included. Most of the previous workers in this field did not incorporate the fuel system dynamics. Open loop model for boiler unit and turbine unit are separately available in literature. In the present attempt the partial models for the boiler and turbine are also incorporated along with developed model for the air heating system, fuel feeding system and furnace system to form the integrated model. The model is simulated on a digital computer (DEC 1090). Extensive tests have been conducted on the model for various system inputs. The behaviour obtained were compared with those of other workers in this area. The various results obtained and the conclusions arrived at are presented. Recommendations for future work are also made.

## CONTENTS

	Page
SYNOPSIS	iv
NOMENCLATURE	vii
CHAPTER 1            INTRODUCTION	1
1.1 Literature Review	4
1.2 Present Work	6
CHAPTER 2            DESCRIPTION OF THE SYSTEM	8
2.1 Introduction	8
2.2 Subsystem I	8
2.3 Subsystem II	11
2.4 Subsystem III	12
CHAPTER 3            MATHEMATICAL MODELS	14
3.1 Introduction to Modelling	14
3.2 Model for Subsystem I	15
3.3 Model for Subsystem II	30
3.4 Model for Subsystem III	38
3.5 Model Structure	52
3.6 Conclusions	53
CHAPTER 4            RESULTS FOR SUBSYSTEM I AND IMPORTANT RESULTS FOR SUBSYSTEMS II AND III	54
4.1 Initialisation	54
4.2 Results for Subsystem I	55
4.3 Important Results for Subsystem II	57
4.4 Important Results for Subsystem III	59
CHAPTER 5            RESULTS FOR COMBINED SYSTEM	61
5.1 Steady State Behaviour	61
5.2 Transient Behaviour for Some Test Inputs	61
5.3 Comments	71

CHAPTER 6	CONCLUSIONS AND SUGGESTIONS FOR FUTURE WORK	72
	6.1 Conclusions	72
	6.2 Suggestions for Future Work	73
APPENDIX I		74
REFERENCES		76

## CHAPTER 1

### INTRODUCTION

The dramatic change in the world energy situation following the steep increase in oil prices since October, 1973 had its impact on India also. The value of import of crude oil and petroleum products went up from Rs. 533 crores in 1973 to Rs.1147 crores in 1975, creating a serious imbalance of payments. As an immediate step, it was decided to introduce measures to curb consumption of petroleum products, specifically for non-essential uses, and identify and implement possibilities of substituting petroleum products with other forms of energy, mainly coal. On the petroleum side, exploration activities have been intensified to locate new oil resources, particularly off-shore. In the coal sector, a comprehensive programme has been evolved and adopted to step-up coal production to meet the increased demands. India is in a slightly better situation as far as the fossil fuel resource is concerned.

In view of the fact that electricity is the most convenient and versatile form of energy, the demand for it in India has been growing at a fast rate. Electricity plays a crucial role in both industrial and agricultural sectors and the productivity in both these sectors is closely linked with adequate availability of power. In view of this, power development has been given high priority in the development

programmes. The main sources of power in the country are thermal, hydro and nuclear fuels. Besides these conventional sources of power, the Ministry of Energy/<sup>Central</sup> is examining the prospects of development of power from non-conventional sources such as geothermal energy, solar energy, wind energy and tidal energy.

Coal based thermal stations contribute about 58 percent of the electricity generation in the country. Considerable economies can be achieved by locating large thermal power stations near colliery pit heads and distributing power from them through extra high voltage transmission lines. It is proposed to initially establish, in a phased manner, super thermal stations in the various regions of the country. Of the total energy, generated, 952,800,00 MWh during 1976-77 thermal energy generated amounts to 572,360,00 MWh. Hydro energy generated during the same period is 347,910,00 MWh and nuclear energy generated was 32,530,00 MWh.

A centrally sponsored programme of establishing inter-state/regional links was included in the Fourth Plan and is being continued in the Sixth Plan also. India has now well connected power systems. Exchange of power is taking place regularly between a large number of states and this generally facilitates better utilisation of the existing capacity. Regional Load Despatch Centres are being established in each

region to facilitate integrated operation of the constituent power systems. It is envisaged that, ultimately, these load-despatch centres would be equipped with on-line computers to control the power stations and power systems automatically.

To design efficient control systems for the power plant thorough understanding of the plant dynamics becomes essential. To study the plant dynamics actual tests on the power plant are highly objectionable because it is not feasible to create major power system disturbances for the purpose of examining system behaviour and effectiveness of proposed strategies or actions. Simulation can be used in such a situation to judge the merits of these strategies under major disturbances. Moreover sensitivity of these strategies to system changes and system model parameters can also be determined. Simulation provides a means of evaluating the system behaviour and helps in predetermining the critical parameters for proper design and operation and their responses to operator actions etc.

Mainly three kinds of problems are studied in dynamic analysis of power systems. First kind of study is carried out for a few seconds of the plant operation. These are called short time problems. The study of instability that may occur when there is a fault on the generating side falls in the first category. Medium time problems are of the second type. The study of response of the system to load changes falls under

this category. The last type of problems are termed as long time problems. Study of start up and shut down comes under the third category. Present work falls under the second category of medium time problem.

The most essential ingredient to the success in the study of the above types of problems is an adequate mathematical model. The model must be reasonably accurate in its representation of the responses of interest. In the present study an attempt has been made to model the complete plant incorporating the already existing but partial models for boiler [7] and turbine [9]. A most general mathematical model to represent a thermal power plant boiler-turbine unit with all the important subsystems are presented in Chapter 3.

### 1.1 Literature Review

In the year 1958 Chien et al.[1] presented a mathematical model and its dynamic analysis for a drum type boiler. An oil fired, single furnace and natural circulation unit was considered for modelling. The model consisting of a number of differential equations was simulated using an electronic differential analyser. He conducted extensive study of the model and a few open loop responses were obtained. But the model was not capable of representing the complicated dynamics of the boiler.

A 200 MW unit of the Philadelphia Electric Company, Crombay is coal fired, twin furnace, controlled circulation reheat boiler. Daniels et al. [17] (1961) developed a mathematical model for the above unit. The primary disturbance input was throttle valve position and the control inputs were coal flow rate, feed water valve position, superheater and reheater burner tilt positions and air flow. Unfortunately, the model did not produce sufficiently accurate responses to be suitable for control system design. In 1965, Thompson presented a very much refined version of the Daniels' model. The primary addition to the model was the use of a large number of elemental volumes to achieve a better approximation to the actual distributed parameter process. Although the model response was significantly improved, it still could not be considered accurate in all respects. In 1967 Nicholson et al. [16] developed an improved version of the model developed by Chien et al. The model described by Anderson et al. [3] in the year 1968 was very similar to that developed by Daniels.

IBM report [10] also presented models for drum type boiler and turbine using lumped parameter technique. Open and closed loop responses were obtained for various control parameters. Kwanty et al. [6] in 1970 developed an extensive model for a boiler-turbine system. The results of the various tests conducted on the model are presented in the report. This model is

relatively simple and accurate and can be used for control system analysis and design.

### 1.2 Present Work

The entire boiler-turbine system is divided into three subsystems for convenience in modelling. Subsystem I consists of the, F.D. fan, air preheaters, economiser and fuel feeding system. ~~Dynamics~~ <sup>The</sup> mathematical model for the subsystem I incorporates the characteristics for the F.D. fan. Empirical relations have been derived to compute the fuel flow rate at various loads, from the actual plant data collected for a period of three months at Panki site. In the furnace dynamics we have incorporated the effect of emissivity of the flue gas also. Subsystem II consists of the boiler drum, downcomer, waterwalls and superheaters. Turbine, reheaters, condenser and feed water heaters together form subsystem III.

An integrated model for the boiler-turbine system is arrived at by coupling the three subsystems together. Models for subsystems II [7] and III [9] were already existing separately. In this thesis, model for subsystem I have been developed and all the models have been combined together. The entire system has then been simulated on a digital computer (DEC 1090). The behaviour of the integrated model for various test inputs have been compared with the results published by various authors. The behaviour of some important system parameters

such as drum pressure, flow through throttle valve, flow at the exit of the MP turbine, reheater steam temperature and pressure etc. have been obtained. These transient behaviours are important in the study of sudden variations in plant inputs.

## CHAPTER 2

### DESCRIPTION OF THE SYSTEM

#### 2.1 Introduction

The thermal power plant selected for the present study is situated at Panki. Panki is a small town, an industrial area, which is about five kilometers away from I.I.T., Kanpur. The erection and commissioning of the two 110 MW units have been done by M/s. Bharat Heavy Electricals Limited and Instrumentation Limited, Kota.

#### 2.2 Subsystem I

##### 2.2.1 Fuel system

The general lay out of the system is as given in Fig. 1. Raw coal from the coal mines is transported to the power plant by trains. Wagon tippler helps lifting and tilting of wagons filled with coal. Wagons are tilted to  $135^{\circ}$  from the vertical to unload the coal by gravity. The unloaded coal is fed to conveyor belts, running over rollers, at a velocity of 2.1 m/sec. by electrically operated vibration feeders. After separating the magnetic particles from the raw coal, by huge magnets, it is sent through sieves. Coal particles of size less than or equal to 20 mm are now fed directly into another conveyor belt leading to Raw Coal Bunkers (R.C.B.). Coal particles bigger than

20 mm size are crushed to the required size before sending to the R.C.B. There are three R.C.B.'s for each of the 110 MW units. Each R.C.B. is of 500 tons capacity.

Crushed coal from the R.C.B. is sent to the ball mills, for pulverisation, by Raw coal feeders. Each of the 110 MW ~~is~~ unit is having three ball mills. Flue gas from the second pass of the furnace is tapped from below the convection superheater. Tapped flue gas is sent to the ball mills along with the coal. Hot flue gas helps pulverising the coal by heating it up. Flue gas is also used as the carrier of the pulverised coal from the ball mills to the classifier. Classifier separates pulverised coal from the bigger particles of coal. Bigger particles of coal are sent back to the mills while pulverised coal particles are carried away by the flue gas to the cyclone separator. Separated pulverised coal, inside the cyclone separator is fed to the Pulverised Coal Bunkers (P.C.B.).

Pulverised coal from the P.C.B. is fed to the P.C. Mixer by the P.C. Feeding system. P.C. Feeding system consists of the following equipments, viz. Shut off side gate, Flap valve, P.C. feeder, Flexible coupling, P.I.V. Chain gear box and electric motor. P.C. feeder is the heart of the system. The body of the P.C. feeder is of cast iron. The upper portion is divided into three chambers by means of partition discs. The top chamber which is the pulverised coal receiving member has

four arms welded on a circular hub. In the middle and bottom chambers there are eight straight arms in each, attached to their respective hubs. All these three hubs are keyed to a vertical shaft which rests on a thrust bearing located at the bottom to enable the flow of pulverised coal from the top and middle chambers to the bottom chamber. They are so arranged so that the flow of pulverised coal is not affected due to the flow of primary air to the mixing nozzle. Though this arrangement prevents the free flow, it will help continuous flow of pulverised coal. There are sixteen P.C. feeders which supply coal to P.C. Mixer at a controlled rate. The rate of flow of pulverised coal is varied by varying the speed of the P.C. feeder. The output from the feeder is proportional to the r.p.m. of the P.C. feeder motor.

### 2.2.2 Air system

Atmospheric air required for combustion of the fuel is pumped into the combustion chamber by Forced Draft (F.D.) fan. Air from the F.D. fan goes to the Air preheater I and then to the Air preheater II. Flue gas flows inside the tubes of preheaters while air flows outside the tubes. During the flow through the preheaters air gets heated mostly by convective heat transfer. Hot air from the Air preheater II enters into the Air distribution box where it gets bifurcated into the primary air and the secondary air. Secondary air directly enters into the combustion

chamber. Primary air mixes with the pulverised coal, coming out of the P.C. feeders, inside the P.C. Mixer. From P.C. Mixer the mixture of primary air and pulverised coal, the fuel ready for combustion, enters the combustion chamber through burners.

#### 2.2.3 Firing system

Combustion chamber is rectangular in shape. There are sixteen coal burners located at the four corners of the combustion chamber tangentially along the periphery of circles, having their centres co-axial with the centre of the combustion chamber. At each corner there are four coal burners, three vapour burners and two oil burners. All the nine nozzle tips are tiltable and are connected to a common tilting mechanism by means of a connecting bar. The coal nozzle tips (four numbers) are provided with jacket air which flows around the coal fuel stream. The burner tips can be tilted to fifteen degrees downwards and fifteen degrees upwards (i.e. a total of thirty degrees) from the horizontal.

### 2.3 Subsystem II

#### 2.3.1 Drum, Downcomer and Waterwalls [7]

Boiler feed pump sends feed water from the feed water tank into the drum. On the way from the feed water tank into the drum it passes through high pressure superheaters and economiser.

Water collected in the drum flows down the downcomer. Downcomer is insulated and is outside the furnace. From the downcomer water enters the waterwall, which is inside the furnace. Risers, also called waterwalls, are arranged on all sides of furnace. Waterwall gets heat mostly by radiation. Inside the waterwall a two phase mixture of water and steam is formed, which flows into the drum through headers.

#### 2.3.2 Superheaters [7]

Steam is collected from the top of the drum, which is at saturated condition. Drum steam first goes to the ceiling superheater and then to the convection superheater. From the convection superheater steam passes through platen superheater and final superheater. Steam properties are controlled between convection and platen superheaters, and between platen and final superheaters by atomeration spray. Ceiling, platen and final superheaters receive heat mostly by radiation.

### 2.4 Subsystem III

#### 2.4.1 Turbine system [9]

Steam from the final superheater passes through a normally open throttle valve, and enters a steam chest. Each steam chest contains four governing valves, which control the steam flow to the turbine. Governing valves are controlled by oil pressure which can be remotely controlled by a pump. Steam

leaving the governing valve is expanded through convergent divergent nozzles and attains very high velocity. High velocity steam gets expanded in two rows of moving blades called the governing stage. The partially expanded steam then gets expanded in High Pressure (H.P.) turbine. Steam from the H.P. turbine is sent for reheating into Triflex reheatater followed by exit reheater. Reheated steam is then expanded in Medium Pressure (M.P.) turbine followed by Low Pressure (L.P.) turbine. The steam exiting from the L.P. turbine is condensed in two condensers each, and the condensate is passed through a series of L.P. feed water heaters.

#### 2.4.2 Feed water heaters and economiser [9]

Condensate, feed water from the condenser is sent through a series of five L.P. feed water heaters. Inside the L.P. feed water heater condensate gets heated by extracted steam from L.P. and M.P. turbines. Hot condensate at the end of L.P. feed water heater enters the Feed water tank. Boiler feed pump pumps the feed water from the tank to H.P. feed water heaters I and II. Feed water gets heated inside the H.P. heaters by the extracted steam from the M.P. turbine and by a small amount of exit steam from the H.P. turbine. Feed water from the heater now enters the economiser. Inside the economiser feed water gets heated finally by flue gas. Hot feed water then passes to the drum. Further details of the system are given in Appendix I.

## CHAPTER 3

### MATHEMATICAL MODELS

#### 3.1 Introduction to Modelling

In an era of increasing electric power utilization, plant availability has become of paramount importance and consequently, its ability to ride smoothly through major as well as minor system disturbances has become essential. Perhaps the most essential step towards better understanding of the generation system and achieving the above is obtaining an adequate mathematical model. Roughly speaking, the basic requirements of such a model are : 1) it must be reasonably accurate in its representation of the responses of interest, 2) it must be relatively simple, and 3) it must bear close resemblance to the physical process, i.e., model parameters should be readily related to physical parameters.

We have adopted a theoretical approach in developing the system model. In this method development of the model is based on some physical laws and also on some semi-empirical relationships. Variables like temperature, velocity etc. that depict the behaviour of components, like waterwalls and super heaters, are continuous functions, of time and space. Dynamics of such components can be adequately described by partial differential equations. Simulation of such a model necessitates considerable

computer time which becomes prohibitive in view of the large number of components to be incorporated in such a model. The entire system is divided or lumped into several sub-systems, across which changes in physical properties take place. The changes across each of the blocks are represented in the form of mathematical equations by applying momentum, mass and energy balance. The mathematical model developed is presented, systematically, in the following articles.

### 3.2 Model for Subsystem I

Subsystem I consists of economiser, F.D. fan, air preheater I, air preheater II, fuel feeding system, and combustion chamber. Feed water pumped out from the feed water tank passes through the high pressure heaters I and II and then through the economiser before it enters the boiler drum. Atmospheric air utilised for combustion of fuelling is sent into the combustion chamber by the F.D. fan. Air coming out of the F.D. fan passes through air pre-heaters I and II where it gets heated by flue gases as explained in Chapter 2. The block diagram showing the flow path is shown in Fig. 1.

#### 3.2.1 Economiser (water side)

The following assumptions were made :

1. Average values of the properties of the water passing through the economiser are assumed to be the exit values

2. Water entering the economiser from the high pressure heater II has the instantaneous properties of the water leaving the high pressure heater II.
3. Water passing through the economiser receives heat mostly by convection.

The rate of heat transfer from the metal tubes to the water is calculated using empirical relations. The flow of water through the economiser is highly turbulent, and the heat transfer relations are of the type [2,3]

$$Q_{EMW} = C_{EMW} W_{HH2}^{0.6} (T_{EM} - T_{EW}) \quad (3.1)$$

where

$Q_{EMW}$  = heat transfer rate from the economiser tube metal to the water (kcals/sec.),

$C_{EMW}$  = a constant to be determined at the time of initialisation,

$W_{HH2}$  = feed water flow rate through the economiser (kg/sec.),

$T_{EM}$  = temperature of the economiser tube metal ( $^{\circ}\text{C}$ ),

$T_{EW}$  = temperature of the feed water leaving the economiser ( $^{\circ}\text{C}$ ).

Initial value for  $T_{EW}$  can be calculated by the following energy balance equation [4] utilizing the data for the resident heat content  $Q_{EMWL}$  collected directly from the plant.

$$Q_{EMW1} = C_{EW} M_{EW} (T_{EW} - T_{HH2}) \quad (3.2)$$

where

- $C_{EW}$  = specific heat of economiser water (kcals/kg °c),
- $M_{EW}$  = resident mass of water inside the economiser (kg),
- $T_{HH2}$  = temperature of water coming out of high pressure heater II (°c).

### 3.2.2 Economiser (gas side)

Similar assumptions (as in 3.2.1) hold good on the gas side of the economiser.

Energy balance on the metal tubes of the economiser lead to the following equation.

$$Q_{EGM} - Q_{EMW} = C_{EM} M_{EM} \frac{d}{dt} (T_{EM}) \quad (3.3)$$

where

- $Q_{EGM}$  = heat transfer rate from flue gases to the economiser metal wall (kcals/sec.),
- $T_{EM}$  = temperature of the economiser tube wall (°c),
- $C_{EM}$  = specific heat of the economiser tube metal (kcals/kg °c),
- $M_{EM}$  = mass of the economiser metal tubes (kg).

Heat transfer rate from flue gas to the economiser metal tube can be calculated using the relation [2,3],

$$Q_{EGM} = C_{EGM} W_G^{0.6} (T_{EG} - T_{EM}) \quad (3.4)$$

where

18

$C_{EGM}$  = a constant to be determined at the time of initialisation,

$W_G$  = flow rate of flue gas through the economiser (kg/sec.),

$T_{EG}$  = temperature of the economiser flue gas ( $^{\circ}\text{C}$ ).

### 3.2.3 F.D. fan

Specific assumptions made during the modelling of F.D. fan are the following :

1. Volume of air flowing out of F.D. fan is linearly related to the external load on the power plant.
2. Atmospheric conditions exist at the inlet to the F.D. fan.

The following empirical formula has been derived from the plant data for calculating the rate of air flow across the F.D. fan.

$$V_{AF} = 2818.0 \times \text{LOAD} + 110.0 \times 10^3 \quad (3.5)$$

where

$V_{AF}$  = Volume flow rate of air across the F.D. fan ( $\text{m}^3/\text{hr}$ ),

LOAD = external load on the power plant (MW).

Mass flow rate of air across the F.D. fan is given by

$$W_{AF} = \rho_{AF} \times V_{AF} \quad (3.6)$$

where

$W_{AF}$  = Mass flow rate of air across the F.D. fan  
(kg/sec.),

$\rho_{AF}$  = density of air coming out of F.D. fan ( $\text{kg/m}^3$ ),

$V_{AF}$  = volume flow rate of air across the F.D. fan  
( $\text{m}^3/\text{sec.}$ ).

### 3.2.4 Air preheater I (air side)

Similar assumptions as in 3.2.1 hold good in the case of air preheater I also.

Heat transfer rate from the tube metal wall of the air preheater I to the air can be found out using the formula

$$Q_{P1MA} = C_{P1MA} W_{AF}^{0.6} (T_{P1M} - T_{P1A}) \quad (3.7)$$

where

$Q_{P1MA}$  = Heat transfer rate from the tube metal to the air (kcals/sec.),

$T_{P1M}$  = temperature of the preheater I tube metal ( $^{\circ}\text{C}$ ),

$T_{P1A}$  = temperature of the preheater I air ( $^{\circ}\text{C}$ ),

$C_{P1MA}$  = a constant to be determined at the time of initialisation.

Initial value for  $T_{P1A}$  can be calculated by the following energy balance equation [4] utilising the data for the resident heat content  $Q_{P1MA1}$  collected directly from the plant.

$$Q_{PLMA} = C_{PLA} (T_{PLA} - T_{AF}) M_{PLA} \quad (3.8)$$

where

$C_{PLA}$  = Specific heat of the air passing through the preheater I (kcals/kg °c),

$T_{AF}$  = temperature of the air coming out of the F.D. fan (°c),

$M_{PLA}$  = resident mass of the air inside the preheater I (kg).

### 3.2.5 Air preheater I (gas side)

On writing down the energy balance for the tube metal of the preheater I we arrive at the following equation

$$Q_{PLGM} - Q_{PLMA} = C_{PLM} M_{PLM} \frac{d}{dt} (T_{PLM}) \quad (3.9)$$

where

$Q_{PLGM}$  = Heat transfer rate from flue gas to the preheater I metal (kcals/sec.),

$C_{PLM}$  = specific heat of the preheater I tube metal (kcals/kg °c),

$M_{PLM}$  = mass of the preheater I tube metal (kg),

$T_{PLM}$  = temperature of the preheater I tube metal (°c).

Heat transfer rate from the flue gas to the preheater I tube metal can be calculated using the formula

$$Q_{PLGM} = C_{PLGM} w_G^{0.6} (T_{PLG} - T_{PLM}) \quad (3.10)$$

where

- $C_{P1GM}$  = a constant to be determined at the time of initialisation,
- $T_{P1G}$  = temperature of the flue gas passing through the preheater I ( $^{\circ}\text{C}$ ),
- $W_G$  = mass flow rate of flue gas passing across the preheater I (kg/sec.).

### 3.2.6 Air preheater II (air side)

It is assumed that the air leaving from the air preheater I and the air entering the air preheater II has got the same properties,

Heat transfer rate from the air preheater II tube metal to the air passing through the preheater II is calculated using the following empirical relation.

$$Q_{P2MA} = C_{P2MA} W_{AF}^{0.6} (T_{P2M} - T_{P2A}) \quad (3.11)$$

where

- $Q_{P2MA}$  = Heat transfer rate from preheater II metal to air (kcals/sec.),
- $C_{P2MA}$  = a constant to be determined at the time of initialisation,
- $T_{P2M}$  = temperature of the preheater II metal ( $^{\circ}\text{C}$ ),
- $T_{P2A}$  = temperature of the preheater II air ( $^{\circ}\text{C}$ ),
- $W_{AF}$  = rate of air flow through the preheater II (kg/sec.).

Initial value for  $T_{P2A}$  can be calculated by the following energy balance equation [4] utilizing the data for the resident heat content  $Q_{P2MA1}$  collected directly from the plant.

$$Q_{P2MA1} = M_{P2A} C_{P2A} (T_{P2A} - T_{P1A}) \quad (3.12)$$

where

$M_{P2A}$  = resident mass of air inside the preheater II (kg),

$C_{P2A}$  = specific heat of air inside the preheater II (kcal/kg °C),

$T_{P1A}$  = temperature of air leaving preheater I (°C).

### 3.2.7 Air preheater II (gas side)

Energy balance on the preheater II tube metal leads to the following equation.

$$Q_{P2GM} - Q_{P2MA} = C_{P2M} M_{P2M} \frac{dT}{dt} (T_{P2M}) \quad (3.13)$$

where

$Q_{P2GM}$  = heat transfer rate from the preheater tube gas to the metal (kcal/sec.),

$C_{P2M}$  = specific heat of the preheater II tube metal (kcal/kg °C),

$M_{P2M}$  = mass of the preheater II tube metal (kg),

$T_{P2M}$  = temperature of the preheater II tube metal (°C).

Heat transfer rate from flue gas to the air preheater II tube metal is calculated using the empirical formula

$$Q_{P2GM} = C_{P2GM} w_G^{0.6} (T_{P2G} - T_{P2M}) \quad (3.14)$$

where

$C_{P2GM}$  = A constant to be determined at the time of initialisation,

$T_{P2G}$  = temperature of the preheater II gas ( $^{\circ}\text{C}$ ).

### 3.2.8 Fuel feeding system

Functioning of the fuel feeding system is explained in Chapter 2. To derive an empirical relationship between the external load on the power plant and number of pulverised coal feeders (P.C. feeders) which are live for that particular load we resorted to the available plant data.

Readings of load against time have been noted continuously for three months. For the above period the number of live P.C. feeders were also noted against time. All the readings have been suitably tabulated and ultimately a graph showing the number of open P.C. feeders versus load in MW have been prepared as shown in Fig. 2.

The following empirical relationship is derived from the graph between load and the number of open P.C. feeders.

$$P_{CF} = LOAD/21.0 + 9.095 \quad (3.15)$$

where

$P_{CF}$  = No. of live or active P.C. feeders,

LOAD = External load on the power plant (MW).

To find out the fuel flow rate into the combustion chamber the following equation is used.

$$W_F = W_{PCF} \times P_{CF} \quad (3.16)$$

where

$W_F$  = Fuel flow rate into the combustion chamber  
(kg/sec.),

$W_{PCF}$  = fuel flow rate through one P.C. feeder (kg/sec.).

### 3.2.9 Combustion chamber

The combustion chamber is assumed to be a black enclosure in which radiation exchange between the entire gas volume and enclosure boundary takes place. Mean beam length approach [5] is used to analyse the situation. Mean beam length is defined as the required radius of a gas hemisphere such that it radiates a flux to the centre of its base equal to the average flux radiated to the area of interest by the actual volume of gas. Mean beam length can be used as a characteristic dimension of the gas volume and regarded as a constant. The recommended equation to calculate the mean beam length is given below [5]

$$L_e = 3.6 V_{FUR} / A_{FUR} \quad (3.17)$$

where

$$\begin{aligned} L_e &= \text{mean beam length (m)}, \\ V_{FUR} &= \text{effective furnace volume (m}^3\text{)}, \\ A_{FUR} &= \text{effective furnace area (m}^2\text{)}. \end{aligned}$$

Emissivity charts have been developed by Hottel [5] from many experimental measurements. The flue gas may contain carbondi-oxide, water vapour carbon monoxide, methane and a few other gases. But it is assumed that except water vapour and carbondi-oxide, all are spectrally transparent gases. It is also assumed that the gas is having uniform temperature inside the chamber.

Graphs are available [5] for  $\epsilon_{H_2O}$  vs  $T_{gw}$  °K and  $\epsilon_{CO_2}$  vs  $T_{gw}$  °K, where  $\epsilon_{H_2O}$  and  $\epsilon_{CO_2}$  are the emissivities of water vapour and carbondi-oxide respectively.  $T_{gw}$  is the gas temperature inside the chamber. These give the total emittance of carbondi-oxide and water vapour obtained experimentally using a mixture with non-absorbing gases so that total pressure of the gas was 1 atmosphere while partial pressures of carbondi-oxide and water were varied.

For a gas mixture other than 1 atmosphere, a pressure broadening correction is to be applied [5]. This is given as a multiplying constant  $C_{CO_2}$  in the case of carbondi-oxide. In

in the case of water vapour the emittance is influenced in a slightly more complex manner by both the partial pressure of the water vapour and the total pressure of the gas mixture. The correction for water vapour  $C_{H_2O}$  is dependant on the mean beam length also.

For our problem  $C_{CO_2}$  and  $C_{H_2O}$  have been estimated from the graphs [5] of  $C_{CO_2}$  vs  $P_{total} + P_{CO_2} + P_{CO_2}^2 / 2.0$ ,  $C_{H_2O}$  vs  $(\frac{P_{total} + P_{H_2O}}{2})$  and  $C_{H_2O}$  vs  $P_{H_2O} L_e$ ,

where

$P_{total}$  = total pressure of the gas,

$P_{H_2O}$  = partial pressure of water vapour,

$P_{CO_2}$  = partial pressure of carbondi-oxide

$C_{CO_2}$  and  $C_{H_2O}$  can be assumed to be constants in our case for the partial pressures inside the combustion chamber are assumed to be constants.

As in the present case if  $CO_2$  and water vapour are both present in the gas mixture, an additional quantity  $\Delta \epsilon$  must be included to account for an emittance reduction resulting from spectral overlap of the carbondi-oxide and water absorption bands. This correction factor is found from the graph [5]

$\Delta \epsilon$  vs  $P_{H_2O} / (P_{CO_2} + P_{H_2O})$ . For a mixture of carbondi-oxide and water vapour in a non-absorbing carrier gas the emittance is then given by

$$\varepsilon_g = C_{CO_2} \varepsilon_{CO_2} + C_{H_2O} \varepsilon_{H_2O} - \Delta \varepsilon \quad (3.18)$$

In the present case empirical relationships have been derived between  $\varepsilon_{CO_2}$  and  $T_{gw}$  as well as  $\varepsilon_{H_2O}$  and  $T_{gw}$ . The equations are presented below.

$$\varepsilon_{H_2O} = 0.29 - 0.0001 (T_{gw} + 273.0) \quad (3.19)$$

$$\varepsilon_{CO_2} = 0.212 - 0.05 (T_{gw} + 273.0)/600.0 \quad (3.20)$$

where

$T_{gw}$  = gas temperature inside the chamber.

The process of combustion of pulverised coal in a furnace is extremely complex. A macroscopic view of the process indicates that if the rate of flow  $W_F$  (kgs./sec.) of coal having a heating value equal to  $C_F$  is burnt, the gas temperature with no heat loss [6] would be

$$T_{gw} = \frac{W_F C_F \eta_B}{C_G W_G} + T_{P2A} \quad (3.21)$$

where

$\eta_B$  = efficiency of burning,

$C_G$  = specific heat of the gas,

$W_G$  = mass rate of flow of flue gas through the furnace (kg/sec.).

Writing down the mass balance inside the combustion chamber we get

$$W_G = W_{AF} + W_F (1 - W_{ASH}) \quad (3.22)$$

where

$W_{ASH}$  = ash content in the pulverised coal,

$W_{AF}$  = mass flow rate of air into the combustion chamber  
(kg/sec.).

The ceiling and convection superheaters are clubbed together and is termed as primary superheater. This forms the first section. Platen and exit superheaters together is also considered as a single unit called the secondary superheater. Both waterwalls and secondary superheater lie in the first pass of the furnace while the primary superheater is in the second pass of the furnace, which receives heat energy mostly by convective heat transfer. Secondary superheater and waterwalls receive heat mostly by thermal radiation from the flue gas.

Taking the heat balance on the gas shows that the net average heat flux being removed at the wall is the gas emission minus the emission from the wall that is absorbed by the gas.

$$Q_{GW} = A_{WS} \sigma [ \epsilon_g (T_{gw} + 273)^4 - \alpha_g (T_{WM} + 273)^4 ] \quad (3.23)$$

where

$Q_{GW}$  = heat transfer rate from flue gas to the waterwalls  
(kcals/sec.),

$A_{WS}$  = effective waterwall surface area ( $m^2$ ),

- $T_{WM}$  = waterwall metal temperature ( $^{\circ}\text{C}$ ),  
 $a_g$  = absorptance of the gas for radiation emitted  
 from the wall at temperature  $T_{WM}$ ,  
 $\sigma$  = Stefan-Boltzmann constant (kcals/sec  $\text{m}^2 \text{ } ^{\circ}\text{K}^4$ ).

Similarly for the secondary superheater, the radiative heat transfer rate from the flue gas to the metal walls can be calculated by the following equation

$$Q_{SM2} = A_{S2} \sigma [\varepsilon_g (T_{gw} + 273)^4 - a_g (T_{SM2} + 273)^4] \quad (3.24)$$

where

- $Q_{SM2}$  = heat transfer rate from flue gas to the secondary superheater metal (kcals/sec.),  
 $A_{S2}$  = effective surface area of the secondary superheater metal exposed to the furnace ( $\text{m}^2$ ),  
 $T_{SM2}$  = temperature of the metal tube of secondary superheater ( $^{\circ}\text{C}$ ).

Due to the considerable heat transfer rates into the waterwalls and primary superheater in the first pass of the furnace the temperature of the flue gas decreases as it leaves the first pass. An energy balance on flue gas in the first pass is done to find out the temperature of the flue gas leaving the first pass. The derived equation is as follows,

$$T_{GWP} = [(T_{gw} + 273)^4 - \frac{(Q_{GW} + Q_{SM2})^{1/4}}{\text{COEF}}] - 273 \quad (3.25)$$

where

30

$T_{GWP}$  = temperature of the flue gas leaving the first pass of the furnace ( $^{\circ}\text{C}$ ),

COEF = a constant to be determined at the time of initialisation.

Heat transfer rate from the flue gas to the primary superheater can be calculated using the empirical relation,

$$Q_{SML} = C_{HMS} w_G^{0.6} (T_{GWP} - T_{SML}) \quad (3.26)$$

where

$Q_{SML}$  = heat transfer rate from the flue gas to the primary superheater (kcals/sec.),

$C_{HMS}$  = a constant to be determined at the time of initialisation,

$T_{SML}$  = temperature of the primary superheater metal ( $^{\circ}\text{C}$ ).

### 3.3 Model for Subsystem II

Subsystem II consists of the drum, downcomer, waterwalls, primary superheater and secondary superheater [7]. All the variables are defined in the Nomenclature.

#### 3.3.1 Drum-Downcomer-waterwalls

Drum-Downcomer-waterwalls system is considered as a single loop in which fluid flow is due to the density changes

only and hence natural circulation exists in the loop. This system is conveniently divided into three separate sections viz. drum, downcomer and waterwalls to facilitate lumped parameter representation [7].

### 3.3.2 Drum

Specific assumptions :

1. The drum is well insulated and heat energy stored in the drum material is negligible.
2. Outlet flow rate of steam from the drum is assumed to be proportional to the square-root of the product of drum pressure and density [8]. This is made possible by assuming an imaginary throttle valve at the outlet of the drum.
3. Feed water is supplied at saturation temperature to the drum and variations of properties of water and steam within the drum are very small.

Mass balance and energy balance on the drum water yield the following equations :

$$(m_{eo} + m_{wo} - m_{ri} - m_{di}) = \frac{d}{dt} (\rho_{drw} V_{drw} + \rho_{drs} V_{drs}) \quad (3.27)$$

and

$$\begin{aligned} & (m_{eo} h_{eo} + m_{wo} h_{wo} - m_{ri} h_{ri} - m_{di} h_{di}) \\ & = \frac{d}{dt} (\rho_{drw} V_{drw} h_{drw} + \rho_{drs} V_{drs} h_{drs}) \end{aligned} \quad (3.28)$$

Following empirical relations are used to determine certain variables which appear in the above equations.

$$V_{dr} = V_{drs} + V_{drw} \quad (3.29)$$

$$\dot{V}_{drw} = C_4 + C_5 (P_{dr} + C_3) \quad (3.30)$$

$$\dot{V}_{drs} = C_{12} + C_{13} (P_{dr} + C_3) \quad (3.31)$$

$$h_{drw} = C_1 + C_2 (P_{dr} + C_3) \quad (3.32)$$

$$h_{drs} = C_{10} + C_{11} (P_{dr} + C_3) \quad (3.33)$$

where  $C_2$ ,  $C_5$ ,  $C_{11}$  and  $C_{13}$  are constants to be determined by using linear fit for the enthalpies and densities from the steam tables.

The steam flow rate out of the drum is calculated by using the formula

$$m_{ri} = C_{throttle} (P_{dr} \dot{V}_{drs})^{\frac{1}{2}} \quad (3.34)$$

where  $C_{throttle}$  = a constant determined at the time of initialisation.

### 3.3.3 Downcomer

Mass, energy and momentum balance on the circulating hot water through the downcomer yield the following equations :

$$(m_{di} - m_{do}) = \frac{d}{dt} (V_d \dot{V}_{do}), \quad (3.35)$$

$$(m_{di} h_{di} - m_{do} h_{do}) = \frac{d}{dt} (V_d \beta_{do} h_{do}), \quad (3.36)$$

and

$$\begin{aligned} 10^4 (P_{dr} - P_{do}) &= \frac{2}{g} \frac{f_d}{D_d} \frac{L_{df}}{A_d^2} \frac{m_{di}^2}{\beta_{di}} + \frac{1}{2g} \frac{m_{di}^2}{A_d^2} \frac{\beta_{di}^2}{\beta_{do}^2} \\ &- \left[ \frac{m_{di}^2}{g A_d^2 \beta_{di}} - \frac{m_{do}^2}{g A_d^2 \beta_{do}} \right] - \beta_{di} L_{db} \frac{L_{df}}{g A_d} \frac{d}{dt} (m_{di}) \end{aligned} \quad (3.37)$$

Empirical relation used to calculate the density of downcomer outlet water is given by

$$\beta_{do} = C_{16}(P_{do} + C_3) + C_{17} (h_{do} - C_{18}) + C_{19} \quad (3.38)$$

### 3.3.4 Waterwalls (water side)

The mass, energy and momentum balance for the water in the waterwalls are as given below :

$$(m_{do} - m_{wo}) = \frac{d}{dt} (V_w \beta_{wo}), \quad (3.39)$$

$$(m_{do} h_{dc} - m_{wo} h_{wo} + Q_w) = \frac{d}{dt} (V_w \beta_{wo} h_{wo}), \quad (3.40)$$

and

$$\begin{aligned} 10^4 (P_{do} - P_{dr}) &= \frac{2f_w}{D_w} \frac{L_{wf}}{A_w^2} \frac{m_{wo}^2}{\beta_{wo}} + \frac{1}{2g} \frac{m_{wo}^2}{A_w^2} \frac{\beta_{wo}^2}{\beta_{do}^2} \\ &- \left[ \frac{m_{do}^2}{g A_d^2 \beta_{do}} - \frac{1}{g A_w^2} \frac{m_{wo}^2}{\beta_{wo}} \right] + \left( \frac{\beta_{do} + \beta_{wo}}{2} \right) L_{wf} \\ &+ \frac{L_{wf}}{g A_w} \frac{d}{dt} (m_{wo}) \end{aligned} \quad (3.41)$$

Empirical relations used to calculate the two-phase friction factor,  $f_w$ , density of the two-phase mixture leaving the waterwall,  $\rho_{wo}$  and the enthalpy of the two-phase mixture leaving the waterwall  $h_{wo}$  are given below.

$$f_w = f_d [1 + 2400 (X/P_{dr})^{0.96}], \quad (3.42)$$

$$\frac{1}{\rho_{wo}} = \frac{X}{\rho_{wos}} + \frac{(1 - X)}{\rho_{wow}}, \quad (3.43)$$

and

$$h_{wo} = X h_{wos} + (1 - X) h_{wow} \quad (3.44)$$

### 3.3.5 Waterwalls (gas side)

Energy balance for the waterwall tube metal yield the following equation :

$$(Q_{gw} - Q_W) = \frac{d}{dt}[C_{WM} \rho_{WM} V_{WM} T_{WM}] \quad (3.45)$$

Heat transfer rate to the two-phase mixture from the waterwall is calculated using the equation

$$Q_W = \text{CONST} (T_{WM} - T_{dr})^3 \quad (3.46)$$

An empirical equation is used to calculate the temperature of the liquid in the waterwalls, which is given by

$$T_{dr} = C_{14} + C_{15} (P_{dr} + C_3) \quad (3.47)$$

### 3.3.6 Superheaters

Superheaters are represented by three sections. The ceiling and convection superheaters together is termed as primary superheater, which is the first section. The third section is the combination of platen and exit superheaters and is called the secondary superheater. The second section is assumed to be a unit which effectively simulates the flow dynamics of the superheater lines. This can be imagined as a connecting link between the primary and secondary superheaters.

### 3.3.7 Primary superheater (steam side)

Mass and energy balance relations for the steam passing through the primary superheater is expressed as

$$(m_{ri} - w_o + w_{DS1}) = \frac{d}{dt} (V_{sl} \dot{f}_{sl}) \quad (3.48)$$

and

$$\frac{d}{dt} (\dot{q}_{sl}) = [Q_{sl} + m_{ri} h_{wos} - w_o h_{sl} + w_{DS1} h_{DS}] \frac{1}{V_{sl}} \dot{V}_{sl} \quad (3.49)$$

The expression for change in enthalpy of superheated steam in the primary superheater can be written as

$$\frac{d}{dt} (h_{sl}) = [\frac{d}{dt}(\dot{q}_{sl}) + \frac{J P_{sl}}{\dot{f}_{sl}} \frac{d}{dt}(\dot{f}_{sl})] \frac{1}{(1 - k_1 J)} \quad (3.50)$$

The pressure in the primary superheater is calculated using the equation

$$P_{sl} = (k_1 h_{sl} - k_2) \dot{V}_{sl} \quad (3.51)$$

### 3.3.8 Primary superheater (gas side)

An energy balance for the primary superheater yield the following equation :

$$(Q_{SML} - Q_{Sl}) = C_{Sl} M_l \frac{d}{dt} (T_{SML}) \quad (3.52)$$

The rate of heat transfer from tubes to the steam is calculated using the expression

$$Q_{Sl} = C_{PS} (W'_o)^{0.8} (T_{SML} - T_{sl}) \quad (3.52)$$

where  $T_{sl}$  is calculated using the equation given below

$$T_{sl} = T_{Hl}(h_{sl} - h_{sTl}) + T_{Rl}(\dot{V}_{sl} - \dot{V}_{sTl}) + T_{sTl} \quad (3.53)$$

### 3.3.9 Connecting link between primary and secondary superheaters

It is assumed that in the steady state flow is proportional to the pressure drop between the superheaters. Thus, we can write :

$$T_{CL} \frac{d}{dt} (W'_o) = k_p (P_{sl} - P_{s2}) - W'_o \quad (3.54)$$

where  $T_{CL}$  = time delay constant for the connecting link (sec.)

### 3.3.10 Secondary superheater (steam side)

Mass and energy balance equations for the steam flowing through the secondary superheater are presented below.

$$(W_o' - W_1 + W_{DS2})/V_{s2} = \frac{d}{dt} (\dot{\gamma}_{s2}) \quad (3.55)$$

and

$$\frac{d}{dt}(q_{s2}) = [Q_{S2} + W_o' h_{s1} + W_{DS2} h_{ds} - W_1 h_{s2}] \frac{1}{\dot{\gamma}_{s2} V_{s2}} \quad (3.56)$$

Expression for the rate of change of enthalpy of steam is given by

$$\frac{d}{dt}(h_{s2}) = [\frac{d}{dt}(q_{s2}) + \frac{J P_{s2}}{\dot{\gamma}_{s2}^2} \frac{d}{dt}(\dot{\gamma}_{s2})] \frac{1}{(1 - k_1 J)} \quad (3.57)$$

The pressure  $P_{s2}$  is calculated from the relation

$$P_{s2} = (k_1 h_{s2} - k_2) \dot{\gamma}_{s2} \quad (3.58)$$

### 3.3.11 Secondary superheater (gas side)

An energy balance on the secondary superheater metal yield the following equation :

$$(Q_{SM2} - Q_{S2}) = C_{S2} M_2 \frac{d}{dt} (T_{SM2}) \quad (3.59)$$

The rate of heat transfer from the tubes to the steam is calculated using the empirical relation

$$Q_{S2} = C_{HS} (W_1)^{0.8} (T_{SM2} - T_{s2}) \quad (3.60)$$

For the superheated steam the temperature is calculated using the expression [7]

$$T_{s2} = T_{H2}(h_{s2} - h_{sT2}) + T_{R2}(\dot{\gamma}_{s2} - \dot{\gamma}_{sT2}) + T_{sT2} \quad (3.61)$$

The flow rate of steam from superheater through the normally open throttle valve is calculated using the expression

$$W_1 = CCA(P_{S2} \beta_{S2})^{\frac{1}{2}} \quad (3.62)$$

### 3.4 Model for Subsystem III

Subsystem III consists of the governing stage of the turbine, high pressure turbine, reheaters, medium pressure turbine, low pressure turbine, feed water heaters and condenser [9]. The model is presented below.

#### 3.4.1 Governing stage of turbine

There are four throttle valves [9] to control the admission of steam to the high pressure turbine. These four valves are followed by a nozzle ring followed by two rows of moving blades with an intervening row of fixed guide blades. These constitute the governing stage of the turbine. Two of these four valves are adjusted to open at the same oil pressures and so both the valves are lumped together into one unit. As a result the steam admission has been modelled through three valves instead of the four valves. The assumptions made at each stage is given in [9]. The mass flow rate through the throttle valve is given by

$$(W_T)_V^2 = \frac{A_T^2}{C_T} \beta_{SS} (P_{SS} - P_{THI}) \quad (3.63)$$

Mass flow rate through the nozzle ring is given by

$$(w_T)_N^2 = C \beta_{THI} (P_{THI} - P_{HP}) \quad (3.64)$$

Assuming that there is no storage in the nozzle ring the flows given by eqns. (3.63) and (3.64) are equal. Hence for a particular load we can derive the expression for the ratio of flow of steam as

$$(w_T)^2 = \frac{A_T^2 C \beta_{THI}}{A_T^2 \beta_{SS} + C_T \beta_{THI} C} \beta_{SS} (P_{SS} - P_{HP}) \quad (3.65)$$

If the pressure ratio across the valve and nozzle combination is less than the critical pressure ( $P_{HP}/P_{SS}$  is less than 0.5054) then sonic conditions exist and the flow is independent of the down stream conditions. In that case flow equation can be expressed as [6]

$$w_T = A_T C_3 \frac{P_{SS}}{\sqrt{T_{SS}}} \quad (3.66)$$

The state relations used for determining nozzle ring steam temperatures obtained by using empirical fits from steam tables are given below.

$$T_{TH1} = 0.5 P_{TH1} + 1.33 H_{TH1} - 620.0, \quad (3.67)$$

$$T_{TH2} = 0.5 P_{TH2} + 1.33 H_{TH2} - 620.0 \quad (3.68)$$

and

$$T_{TH3} = 0.5 P_{TH3} + 1.33 H_{TH3} - 620.0 \quad (3.69)$$

Temperatures of steam streams at the exit of the nozzle rings are calculated using the following equations.

$$T_{HP1} = T_{TH1} \left( \frac{P_{HP}}{P_{TH1}} \right)^{\frac{n-1}{n}}, \quad (3.70)$$

$$T_{HP2} = T_{TH2} \left( \frac{P_{HP}}{P_{TH2}} \right)^{\frac{n-1}{n}} \quad (3.71)$$

and

$$T_{HP3} = T_{TH3} \left( \frac{P_{HP}}{P_{TH3}} \right)^{\frac{n-1}{n}} \quad (3.72)$$

Following empirical relations are used to determine the enthalpies of the exiting steam from the nozzle ring

$$H_{HP1} = -0.3 P_{HP} + 0.617 T_{HP1} + 527.6, \quad (3.73)$$

$$H_{HP2} = -0.3 P_{HP} + 0.617 T_{HP2} + 527.6 \quad (3.74)$$

and

$$H_{HP3} = -0.3 P_{HP} + 0.617 T_{HP3} + 527.6 \quad (3.75)$$

### 3.4.2 High pressure turbine

High pressure turbine impulse blades are assumed to ideally convert the kinetic energy into work. Further, it is also assumed that the relationship between enthalpy, specific volume, and pressure for the superheated steam follows Callendar's empirical relationship for all non-constant pressure processes [10].

The flow through the high pressure turbine is related to the pressure drop across it. The expression used is

$$(W_T)^2 = K_1 \rho_{HP} (P_{HP} - P_{CR}) \quad (3.76)$$

The rate of change of outlet flow of H.P. turbine with a change in the inlet flow into the turbine is expressed as

$$\frac{d}{dt} (W_{CR}) = \frac{(1 - c_o) W_T - W_{CR}}{T_o} \quad (3.77)$$

Expansion of steam in the turbine is assumed to be isentropic ( $n = 1.3$ ). Temperature and enthalpy of the exiting steam from the H.P. turbine are given by

$$T_{CR} = T_{HP} \left( \frac{P_{CR}}{P_{HP}} \right)^{\frac{n-1}{n}} \quad (3.78)$$

and

$$H_{CR} = 0.5934 P_{CR} + 0.65 T_{CR} + 534.069 \quad (3.79)$$

The overall efficiency,  $\eta_{HP}$ , of the H.P. turbine is corrected by a factor,  $\eta_F$ , to get the actual efficiency,  $\eta_{HPA}$ , of the turbine. Correction is done to compensate for the effects of stage leakages, root and tip interference losses and rotational losses which increase with the flow rate. Actual efficiency and the actual reheat enthalpy are then given by

$$\eta_{HPA} = \eta_{HP} \eta_F \quad (3.80)$$

where  $\eta_F = \frac{(W_{CR}/W_R) - W_L}{(W_{CR}/W_R)(1-W_L)}$  (3.80A)

and

$$H_{CRA} = H_{HP} - \eta_{HPA} (H_{HP} - H_{CR}) \quad (3.81)$$

The power produced by the H.P. turbine in terms of the flow rate and enthalpy drop in the H.P. turbine is expressed as

$$POW_1 = 0.0042 W_T \eta_{HPA} (H_{HP} - H_{CR}) \quad (3.82)$$

#### 3.4.4 Triflex reheater (steam side)

Mass, momentum and energy balance on the steam side lead to the following equations :

$$W_{CR} - W_{ROL} = \frac{d}{dt} (\rho_{R1} V_{R1}), \quad (3.83)$$

$$P_{CR} - P_{ROL} = F_{R1} \frac{W_{CR}^2}{\rho_{R1}} + \frac{L_1}{A_1 g} \frac{(1-C_o)W_T - W_{CR}}{T_o} \quad (3.84)$$

and

$$\frac{1}{\gamma} \frac{d}{dt} (M_{R1} H_{ROL}) = Q_{RS1} - H_{ROL} W_{ROL} + H_{CR} V_{CR} \quad (3.85)$$

Temperature of the steam in the Triflex reheat and the heat added to the steam from the metal walls are given by

$$T_{RS1} = 0.785(P_{ROL} - 24.47) + 1.81(H_{ROL} - 772.0) + 397.0 \quad (3.86)$$

and

$$Q_{RS1} = C_{RMS1} (W_{ROL})^{0.8} (T_{RML} - T_{RS1}) \quad (3.87)$$

A large volume of steam is occupied by the reheat器 and so there is a storage effect in it. As a result we can consider it as a tank across which the changes in flow are approximated by a first order transfer function.

The following equation is derived to represent the rate of change of steam flow leaving the Triflex reheat器.

$$\frac{d}{dt} (W_{RI2}) = \frac{W_{CR} - W_{RI2}}{T_7} \quad (3.88)$$

#### 3.4.5 Triflex reheat器 (gas side)

The energy storage in the Triflex reheat器 leads to the following equation.

$$Q_{RG1} - Q_{RS1} = C_{TM1} M_1 \frac{d}{dt} (T_{RM1}) \quad (3.89)$$

#### 3.4.6 Exit reheat器 (steam side)

Mass, momentum and energy balance equations for the steam in the exit reheat器 are

$$W_{RI2} - W_{R02} = \frac{d}{dt} (F_{R2} V_{R2}), \quad (3.90)$$

$$P_{RI2} - P_{R02} = F_{R2} \frac{W_{RI2}}{A_2 g} + \frac{L_2}{A_2 g} \frac{d}{dt} (W_{RI2}) \quad (3.91)$$

and

$$\frac{1}{\gamma} \frac{d}{dt} (M_{R2} H_{R02}) = Q_{RS2} + H_{RI2} W_{RI2} - H_{R02} W_{R02} \quad (3.92)$$

The empirical relations used for determining exit reheater temperature and the heat added to steam in the exit reheater are

$$T_{RS2} = 0.96 (P_{R02} - 23.12) + 2.05 (H_{R02} - 845.0) + 535.0 \quad (3.93)$$

and

$$Q_{RS2} = C_{RMS2} (W_{R02})^{0.8} (T_{RM2} - T_{RS2}) \quad (3.94)$$

As in the case of Triflex reheater, the rate of change of flow of steam out of the exit reheater is given by

$$\frac{d}{dt} (W_{RQ2}) = \frac{W_{RI2} - W_{R02}}{T_8} \quad (3.95)$$

#### 3.4.7 Exit reheater (gas side)

The energy storage in the metal tube wall of exit reheater is given by the following equation

$$Q_{RG2} - Q_{RS2} = C_{TM2} M_2 \frac{d}{dt} (T_{RM2}) \quad (3.96)$$

#### 3.4.8 Medium pressure turbine

Inlet flow to the M.P. turbine is supplemented by attemperation flow to control the temperature. This is also incorporated in the model. Inlet flow into the M.P. turbine is given by

$$W_{MPI} = W_{R02} + W_{ATMP} \quad (3.97)$$

Energy balance for attemperator is given by the expression

$$W_{R02} H_{R02} = H_{MPI} W_{MPI} + W_{ATMP} H_{ATMP} \quad (3.98)$$

The flow through each turbine is related to their respective inlet and outlet pressures by the following expressions.

$$w_{MPI}^2 = K_2 \beta_{R2} (P_{MPI} - P_{MP1}), \quad (3.99)$$

$$w_{MP1}^2 = K_3 \beta_{MP1} (P_{MP1} - P_{MP2}), \quad (3.100)$$

$$w_{MP2}^2 = K_4 \beta_{MP2} (P_{MP2} - P_{MP3}), \quad (3.101)$$

and

$$w_{MP3}^2 = K_5 \beta_{MP3} (P_{MP3} - P_{MPO}). \quad (3.102)$$

The rate of change of flow in each of the turbine inlet is described by,

$$\frac{d}{dt}(w_{MP1}) = \frac{(1 - c_4) w_{MPI} - w_{MP1}}{T_2}, \quad (3.103)$$

$$\frac{d}{dt}(w_{MP2}) = \frac{(1 - c_5) w_{MP1} - w_{MP2}}{T_3}, \quad (3.104)$$

$$\frac{d}{dt}(w_{MP3}) = \frac{(1 - c_6) w_{MP2} - w_{MP3}}{T_4} \quad (3.105)$$

and

$$\frac{d}{dt}(w_{MPO}) = \frac{(1 - c_7) w_{MP3} - w_{MPO}}{T_5} \quad (3.106)$$

Temperatures at each stage of the turbine are determined using the following equations

$$T_{MP1} = T_{MPI} \left( \frac{P_{MP1}}{P_{MPI}} \right)^{\frac{n-1}{n}}, \quad (3.107)$$

$$T_{MP2} = T_{MP1} \left( \frac{P_{MP2}}{P_{MP1}} \right)^{\frac{n-1}{n}}, \quad (3.108)$$

$$T_{MP3} = T_{MP2} \left( \frac{P_{MP3}}{P_{MP2}} \right)^{\frac{n-1}{n}} \quad (3.109)$$

and

$$T_{MPO} = T_{MP3} \left( \frac{P_{MPO}}{P_{MP3}} \right)^{\frac{n-1}{n}} \quad (3.110)$$

Empirical relations used to find out the enthalpy of steam at the exit of each M.P. turbine stage are presented below.

$$H_{MP1} = -0.35 P_{MP1} + 0.52 T_{MP1} + 571.8, \quad (3.111)$$

$$H_{MP2} = -0.5 P_{MP2} + 0.51 T_{MP2} + 580.4, \quad (3.112)$$

$$H_{MP3} = -0.636 P_{MP3} + 0.5 T_{MP3} + 584.5 \quad (3.113)$$

and

$$H_{MPO} = -1.36 P_{MPO} + 0.48 T_{MPO} + 592.18 \quad (3.114)$$

Efficiency correction factor for each stage is calculated using the following equations :

$$\eta_{FL} = \frac{\left( \frac{W_{MP1}}{W_R} \right) - W_L}{\left( \frac{W_{MP1}}{W_R} \right) (1 - W_L)}, \quad (3.115)$$

$$\eta_{F2} = \frac{\left(\frac{W_{MP2}}{W_R}\right) - w_L}{\left(\frac{W_{MP2}}{W_R}\right)(1 - w_L)}, \quad (3.116)$$

$$\eta_{F3} = \frac{\left(\frac{W_{MP3}}{W_R}\right) - w_L}{\left(\frac{W_{MP3}}{W_R}\right)(1 - w_L)} \quad (3.117)$$

and

$$\eta_{F4} = \frac{\left(\frac{W_{MP4}}{W_R}\right) - w_L}{\left(\frac{W_{MP4}}{W_R}\right)(1 - w_L)} \quad (3.118)$$

Actual efficiencies are determined using the following equations,

$$\eta_{MP1} = \eta_{MP} \eta_{F1}, \quad (3.119)$$

$$\eta_{MP2} = \eta_{MP} \eta_{F2}, \quad (3.120)$$

$$\eta_{MP3} = \eta_{MP} \eta_{F3} \quad (3.121)$$

and

$$\eta_{MP4} = \eta_{MP} \eta_{F4} \quad (3.122)$$

Actual enthalpies are determined as follows :

$$H_{MP1A} = H_{MPI} - \eta_{MP1} (H_{MPI} - H_{MPL}), \quad (3.123)$$

$$H_{MP2A} = H_{MP1A} - \eta_{MP2} (H_{MP1A} - H_{MP2}), \quad (3.124)$$

$$H_{MP3A} = H_{MP2A} - \eta_{MP3} (H_{MP2A} - H_{MP3}) \quad (3.125)$$

and

$$H_{MPOA} = H_{MP3A} - \eta_{MPO} (H_{MP3A} - H_{MPO}) \quad (3.126)$$

Power generated by each turbine is given by the following expressions

$$POW_2 = 0.0042 W_{MP1} \eta_{MP1} (H_{MP1} - H_{MP1}), \quad (3.127)$$

$$POW_3 = 0.0042 W_{MP2} \eta_{MP2} (H_{MP1A} - H_{MP2}), \quad (3.128)$$

$$POW_4 = 0.0042 W_{MP2} \eta_{MP3} (H_{MP2A} - H_{MP3}) \quad (3.129)$$

and

$$POW_5 = 0.0042 W_{MP3} \eta_{MP4} (H_{MP3A} - H_{MPO}) \quad (3.130)$$

### 3.4.9 Low pressure turbine

Exit from this turbine goes to the condenser. Extractions are lumped into one extraction [9] and is assumed to take place at the end of this turbine. Rate of change of L.P. turbine exit flow is given by the expression

$$\frac{d}{dt} (W_{LPO}) = \frac{(1 - c_8) W_{MPO} - W_{LPO}}{T_6} \quad (3.131)$$

Actual efficiency of the L.P. turbine is calculated as below

$$\eta_{LPA} = \eta_{LP} \eta_{F5} \quad (3.132)$$

where  $\eta_{F5}$ , the efficiency correction factor is given by

$$\eta_{F5} = \frac{\left(\frac{W_{LPO}}{W_R}\right) - W_L}{\left(\frac{W_{LPO}}{W_R}\right)(1 - W_L)} \quad (3.133)$$

Actual enthalpy of steam leaving the L.P. turbine and the power produced by the L.P. turbine are given by the following equations.

$$H_{LPOA} = H_{MPOA} - \eta_{LPA} (H_{MPOA} - H_{LPO}) \quad (3.134)$$

and

$$POW_6 = 0.0042 W_{MPO} \eta_{LPA} (H_{MPOA} - H_{LPO}) \quad (3.135)$$

### 3.4.10 Condenser [9]

Heat flow rate from the metal to the cooling water is given by

$$Q_{MW} = C_{CMW} (W_{CW})^{0.6} (T_{CM} - T_{CW}) \quad (3.136)$$

An energy balance of the fluid inside the condenser is used to calculate the enthalpy of the condensate exiting from the condenser. The expression used is

$$H_{CO} = H_{LPO} - Q_{SM}/W_{LPO} \quad (3.137)$$

Energy balance on the metal wall yields the following equation

$$Q_{SM} - Q_{MW} = C_{CM} M_3 \frac{d}{dt} (T_{CM}) \quad (3.138)$$

### 3.4.11 Low pressure heaters

The model developed for the L.P. heater No. I is represented by the following equations.

$$Q_{LH1SM} - Q_{LH1MW} = C_{HM1} M_4 \frac{d}{dt} (T_{HM1}), \quad (3.139)$$

$$Q_{LH1MW} = C_{HMW1} (w_{LH1})^{0.6} (T_{HM1} - T_{HW1}) \quad (3.140)$$

and

$$H_{LH1O} = H_{CO} + Q_{LH1MW}/w_{LH1} \quad (3.141)$$

The equations derived to represent the L.P. heater No. II are :

$$Q_{LH2SM} - Q_{LH2MW} = C_{HM2} M_5 \frac{d}{dt} (T_{HM2}), \quad (3.142)$$

$$Q_{LH2MW} = C_{HMW2} (w_{LH2})^{0.6} (T_{HM2} - T_{HW2}) \quad (3.143)$$

and

$$H_{LH2O} = H_{LH1O} + Q_{LH2MW}/w_{LH2} \quad (3.144)$$

L.P. heater No. III is represented by the following equations :

$$Q_{LH3SM} - Q_{LH3MW} = C_{HM3} M_6 \frac{d}{dt} (T_{HM3}), \quad (3.145)$$

$$Q_{LH3MW} = C_{HMW3} (w_{LH3})^{0.6} (T_{HM3} - T_{HW3}) \quad (3.146)$$

and

$$H_{LH3O} = H_{LH2O} + Q_{LH3MW}/w_{LH3} \quad (3.147)$$

The following equations constitute the model for the L.P. heater No. IV.

$$Q_{LH4SM} - Q_{LH4MW} = C_{HM4} M_7 \frac{d}{dt} (T_{HM4}), \quad (3.148)$$

$$Q_{LH4MW} = C_{HMW4} (w_{LH4})^{0.6} (T_{HM4} - T_{HW4}) \quad (3.149)$$

and

$$H_{LH4O} = H_{LH3O} + Q_{LH4MW}/w_{LH4} \quad (3.150)$$

### 3.4.12 High pressure heaters

Equations derived to represent the H.P. heater No. I are :

$$Q_{HH1SM} - Q_{HH1MW} = C_{HM5} M_8 \frac{d}{dt} (T_{HM5}), \quad (3.151)$$

$$Q_{HH1MW} = C_{HMW5} (w_{HH1})^{0.6} (T_{HM5} - T_{HW5}) \quad (3.152)$$

and

$$H_{HH1O} = H_{LH4O} + Q_{HH1MW}/w_{HH1} \quad (3.153)$$

The following three equations represent the model for the H.P. heater II :

$$Q_{HH2SM} - Q_{HH2MW} = C_{HM6} M_9 \frac{d}{dt} (T_{HM6}), \quad (3.154)$$

$$Q_{HH2MW} = C_{HMW6} (w_{HH2})^{0.6} (T_{HM6} - T_{HW6}) \quad (3.155)$$

and

$$H_{HH2O} = H_{HH1O} + Q_{HH2MW}/w_{HH2} \quad (3.156)$$

LIBRARY  
CENTRAL LIBRARY  
 Acc. No. **59255**

### 3.5 Model Structure

The structure of the non-linear ordinary differential equations is of the form

$$\dot{\bar{X}} = f(\bar{X}, \bar{Y}, \bar{U}) \quad (3.157)$$

where  $\bar{X}$  is the state vector given by

$$\begin{aligned} \bar{X}^T = & (T_{EM}, T_{P1M}, T_{P2M}, P_{dr}, V_{drw}, P_{do}, m_{di}, X, T_{WM}, \\ & m_{W3}, h_{do}, f_{sl}, h_{s1}, f_{s2}, h_{s2}, W_o, T_{SM1}, T_{SM2}, \\ & W_{CR}, V_{R1}, H_{R01}, T_{RM1}, W_{RI2}, J_{R2}, H_{R02}, W_{R02}, \\ & T_{RM2}, W_{MP1}, W_{MP2}, W_{MP3}, W_{MPO}, T_{CM}, T_{HML}, T_{HM2}, \\ & T_{HM3}, T_{HM4}, T_{HM5}, T_{HM6}). \end{aligned}$$

$\bar{Y}$ , the auxiliary variables are given by

$$\bar{Y} = G(\bar{X}, \bar{U}) \quad (3.158)$$

$\bar{U}$  is the control vector defined by

$$\bar{U}^T = (m_{eo}, W_F, W_{AF}, A, LOAD)$$

Substituting for  $\bar{Y}$  from equation (3.158) in equation (3.157) we can rewrite as

$$\dot{\bar{X}} = F(\bar{X}, \bar{U}) \quad (3.159)$$

where  $\tilde{F}$  denotes the new functional dependence.

To solve the above set of equation a computer programme was developed. These equations were solved on a digital computer (DEC:1090) using Runge-Kutta integration technique. The transient responses of the complete system for step changes in control parameters were obtained. The results of the tests conducted are discussed in Chapter 5.

### 3.6 Conclusions

In this chapter we have presented the model developed for the entire system which consists of forty first order differential equations and one hundred and seventeen algebraic equations. In the present model we have included all of the important components of the plant. But it was impossible to include the dynamics of the ball-mills used for pulverising the coal due to the lack of sufficient data. Further, the ball-mills are adjusted (in the present plant set-up) manually from time-to-time.

## CHAPTER 4

### RESULTS FOR SUBSYSTEM I AND IMPORTANT RESULTS FOR SUBSYSTEMS II AND III

#### 4.1 Initialisation

A mathematical model developed for the Ranki thermal power plant was presented in Chapter 3. The steady state values of the state variables are to be determined as a first step for any further study of the behaviour of the model. Obtaining the steady state operating variables for the plant dynamics is termed as initialisation. There are two methods available for initialisation. In the first method the left hand side of the equation (3.158) is equated to zero. The new set of equations are now solved using a suitable elimination technique to find out the steady state values. Second method is a simpler method in which operating data are collected from the plant to use as a starting point in the integration scheme of the equation (3.158). Latter method is adopted in the present attempt.

All the three subsystems were simulated to obtain steady state values using fourth order Runge-Kutta method for integration. In our case the integration was terminated when the difference between the successive values of the state variables is of the order of 0.001. The steady state values obtained

for the complete system at a load of 100 MW is tabulated in the next chapter. Results of the individual tests conducted on the subsystem I, subsystem II [7] and subsystem III [9] are presented below.

#### 4.2 Results for Subsystems I

Two tests have been conducted on the model. 20 percent step decrease have been made on the fuel flow rate to get the transient responses. A 20 percent step decrease in air flow from steady state have been made to conduct the second test. Results obtained are discussed below.

##### (a) 20 percent step decrease in fuel flow rate

The responses obtained are plotted in Fig. 3. As the fuel flow rate is suddenly decreased the temperature of the flue gas also undergoes a sharp decrease initially. This is quite evident from equation (3.21). After the initial jump the temperature very slowly decreases and assumes a new steady state value. We can note a similar trend in the case of the temperature ( $T_{GWP}$ ) of flue gas entering the second pass of the furnace. The emissivity of the gas,  $\epsilon_G$  increases as the temperature of the gas decreases, in the operating region, which is the expected trend for emissivity. Temperature of the air leaving the air preheater II,  $T_{B2A}$  gradually decreases as the fuel flow is decreased. Earlier we have noted the decrease in temperature

of the flue gas entering the second pass of the furnace in which preheaters are located. Due to the decrease in flue gas temperature the heat transfer rate from the flue gas to the air also decreases. Hence ultimately the temperature of the air in the air preheater II also decreases.

(b) 20 percent step decrease in air flow rate

Responses obtained on conducting a 20 percent step decrease in air flow rate from the steady state are presented in Fig. 4. Temperature of the flue gas,  $T_{gw}$  suddenly increases to a high value and then gradually decreases to attain a steady state value. It is assumed that complete combustion takes place inside the combustion chamber. There is a momentary decrease in the rate of flow of flue gas as the air flow rate is decreased. Due to this heat generation rate remaining the same, heat transfer rate into the waterwall metal decreases. So that the temperature of the flue gas may suddenly increase. When the system stabilises the high flue gas temperature gradually decreases to a steady state value. The flue gas entering the second pass of the furnace is also having the same trend as that of the flue gas in the first pass of the furnace. The sudden decrease and then the gradual increase in emissivity is quite expected due to the sudden increase and then the gradual decrease in the flue gas temperature. Air leaving the air preheaters I and II decreases suddenly at first and then gradually decreases to

attain a new steady state value. As we have noted earlier decrease in air flow rate decreases the flue gas flow rate. But flue gas flow rate is proportional to the heat transfer rate from the flue gas to the metal walls. This results in a decrease in the heat transfer rate from the metal wall to the air passing through the preheaters. This ultimately results in the decrease of temperatures leaving the air preheaters I and II.

#### 4.3 Important Results for Subsystem II [7]

Three tests have been conducted on the model for the subsystem II. The results obtained are discussed below.

##### (a) 20 percent step increase in fuel flow rate

This step change is effected by increasing the input flow rate,  $W_F$ . The responses obtained are presented in Fig. 5. With the increase in fuel flow rate there will be an expected increase in steaming rate  $W_1$ . Increase in fuel flow rate increases the waterwall temperature  $T_{WM}$ . As  $W_1$  increases the drum pressure  $P_{dr}$  increases. A decreasing trend in the mass flow rates  $m_{di}$  and  $m_{wo}$  is noted. This decrease is due to the increase in friction losses in the downcomer and waterwalls. The decrease in  $m_{di}$  is rapid as compared to  $m_{wo}$ . Thus there is a net increase in mass flow into the drum from downcomer water-wall loop. This causes an initial increase in the volume of

the drum water since the feed water flow rate and the throttle valve opening are kept constant. This increase in drum water is called swelling effect. Due to the increase in fuel combustion, the temperature of the super heated steam  $T_{s1}$  and  $T_{s2}$  increases. Since the outlet throttle valve opening area A is kept constant during this test, the additional steam produced has to flow through the same area hence this causes a pressure build up.

(b) 20 percent step increase in feed water flow rate

The responses obtained in this case are presented in Fig. 6. As feed water flow rate increases volume of drum water increases. Pressure in the drum  $P_{dr}$  increases gradually on account of the increase in drum water. The increased drum pressure propagates down-stream causing  $P_{s1}$  and  $P_{s2}$  to increase in primary and secondary superheaters respectively. On account of the influx of the feed water the mass flow rate of the water in the down-comer,  $m_{di}$  increases initially till about 5 seconds due to the increase in drum pressure, but decreases afterwards due to the increased friction losses. Mass flow rate of two phase mixture  $m_{wo}$  at waterwalls outlet decreases initially and is again due to the increased friction losses in waterwalls. The increased mass flow rate of steam  $W_1$  through the throttle valve is due to the increase in pressure  $P_{s2}$  resulting from equation (3.62).

(c) 20 percent step increase in throttle valve opening area, A.

The responses for this test are given in Fig. 7. With a step increase in throttle valve area there is an initial sudden increase in steam flow rate,  $W_1$ . This causes the rapid initial drop in throttle pressure  $P_{s2}$ . This is explained by the fact that the friction losses increase in the superheater while the drum pressure  $P_{dr}$  does not change rapidly (not shown in the Fig.). The rapid decrease in temperature  $T_{s2}$  is on account of the assumption made in equation (3.61) that is due to its dependence on  $h_{s2}$  and density of steam in the secondary superheater.  $T_{s1}$  also gradually decreases as time elapses.

#### 4.4 Important Results for Subsystem III [9]

Model responses for a load drop of 10 MW are discussed in this article. For obtaining these the total input flow to turbine,  $W_T$  was decreased by a step to its new value at 80 MW. The various responses obtained are plotted and are presented in Fig. 8.

The curve for the Triflex reheat outlet flow rate,  $W_{R01}$ , shows that  $W_{R01}$  goes down for about six seconds initially and then stabilises. This is because of the large volume involved in the Triflex reheat it behaves just like a storage tank. Reheat outlet pressure,  $P_{R01}$  also decreases as shown by the curve for  $P_{R01}$ .  $P_{R01}$  is dependant on the inlet pressure to the

rheater, the flow and density. But the inlet pressure to the reheater,  $P_{CR}$  and the inflow rate,  $V_{CR}$  go down. So the decrease in  $P_{R01}$  is justified. As  $P_{R01}$  goes down  $T_{RS1}$  also follows the same trend. The flow at the outlet of the M.P. turbine,  $V_{MP1}$  decreases initially and then stabilises to a new value. The pressure at the exit of the first M.P. turbine,  $P_{MP1}$  is affected by the inlet pressure to the turbine, the flow passing through it and the density of the steam. The pressure first goes down because of the effect of decrease in inlet pressure to the M.P. turbine, but as flow also goes down and there is only a marginal decrease in the steam density, the pressure goes up as can be seen from the equation (3.99). The temperature of the steam at the exit of the M.P. turbine follows a similar trend due to its dependence on pressure and also due to the effect of second reheater enthalpy variation. The curve for  $T_{MP1}$  shows the variation of the temperature of the steam at the exit of the M.P. turbine. The heat transfer rate from feed water heater metal to the water (both for L.P. Heater and H.P. Heater) shows a decreasing trend which can be explained by the fact that as the load is decreased the quantity of steam extracted also goes down. As a result less steam condenses on the tubes resulting in lesser heat transfer to the feed water passing through these tubes.

## CHAPTER 5

### RESULTS FOR THE COMBINED SYSTEM

#### 5.1 Steady State Behaviour

All the three subsystems are combined together to get the complete model of the thermal power system. The model is simulated to get the steady state values of the various operating variables. Steady state values obtained are given in the Table 5.1. The units of the variables are described in the Nomenclature.

The tests conducted on the model and results obtained in each case are discussed below.

#### 5.2 Transient Behaviour for Some Test Inputs

##### 5.2.1 20 percent step increase in fuel flow rate, $W_F$

Transient responses obtained are presented in Figs. 12 and 13. (Capital letters are used for notations of parameters in the Figs.). As the fuel flow rate is increased suddenly heat transfer rate from the flue gas to the waterwall also increases rapidly. This leads to a sudden increase in the waterwall metal temperature as shown by the curve c of Fig. 13. But as time elapses more heat is being carried by the flow of water. Thus  $T_{WM}$  settles down to a slightly elevated temperature in due course of time as the rate of flow of heat from the elevated furnace

Table 5.1

Operating Variable	Operating Level	Operating Variable	Operating Level
T <sub>dr</sub>	335.6	P <sub>MP2</sub>	31.3
m <sub>ri</sub>	94.8	P <sub>MP3</sub>	29.1
P <sub>dr</sub>	139.0	P <sub>MPO</sub>	28.2
m <sub>di</sub>	674.7	W <sub>R01</sub>	97.2
T <sub>WM</sub>	368.8	W <sub>MP1</sub>	92.0
m <sub>wo</sub>	674.7	W <sub>CR</sub>	97.0
T <sub>s1</sub>	355.4	W <sub>MP2</sub>	90.2
T <sub>s2</sub>	529.8	W <sub>MP3</sub>	88.3
P <sub>s1</sub>	140.9	W <sub>MPO</sub>	84.2
P <sub>s2</sub>	130.8	T <sub>MP1</sub>	567.0
W <sub>1</sub>	105.5	T <sub>MP2</sub>	556.0
P <sub>CR</sub>	53.5	T <sub>MP3</sub>	542.0
P <sub>R01</sub>	51.5	T <sub>MPO</sub>	536.0
T <sub>RS1</sub>	541.0	T <sub>LPO</sub>	45.0
T <sub>CR</sub>	388.5	Q <sub>L1MW</sub>	1683.0
T <sub>RS2</sub>	647.0	Q <sub>H1MW</sub>	3104.0
P <sub>R02</sub>	49.4	T <sub>P1A</sub>	155.7
W <sub>R02</sub>	97.2	T <sub>P2A</sub>	325.6
P <sub>MP1</sub>	33.2	T <sub>EW</sub>	283.4
W <sub>HH2</sub>	107.0	ε <sub>G</sub>	0.2118

temperature becomes equal to the rate of heat carried away by the flowing water in the waterwall. As  $T_{WM}$  increases more steam is generated in the waterwall tubes. The two phase mixture with higher steam content (and consequently lesser water content) will flow to the drum resulting in a higher rate of circulation in the downcomer-waterwall loop. This is shown by the curves e and f (Fig. 13). As per assumption, the steam outlet from the drum is considered to be through an imaginary throttle valve of constant opening area. This results in higher rate of steam flow into the drum through the waterwall and, consequently, higher drum pressure  $P_{dr}$  as shown in Fig. 13(a). As  $T_{dr}$  and  $P_{dr}$  are related by equation (3.47),  $T_{dr}$  will also have a rising trend. Afterwards, as  $P_{dr}$  gradually stabilises  $T_{dr}$  also follows the trend of  $P_{dr}$ . Trends of temperatures of steam in primary superheater,  $T_{s1}$  and secondary superheater  $T_{s2}$  and their pressures  $P_{s1}$  and  $P_{s2}$  are given by curves d, g, h and i respectively. As the steam generation is increased more steam flows through the superheaters. But the throttle valve after the secondary superheater is kept at the same area of opening. Due to increased fuel flow rate, the superheater temperatures also increase because the superheaters are receiving heat from the furnace. Consequently, it will add to the increase in steam pressures and temperatures ( $P_{s1}$ ,  $P_{s2}$ ,  $T_{s1}$  and  $T_{s2}$ ) of the superheaters. So there is an initial pressure building tendency and temperature increasing tendency inside the superheaters. As  $P_{s2}$  increases

initially the steam flow rate  $W_1$  also increases initially. All the parameters show a stabilising trend after the initial change from the steady state values. The trends of the various parameters obtained in [7] are quite similar to the trend obtained in the present study, for the initial period of time, as shown in Fig. 5. In the present case as time elapses there is a stabilising trend. But in Srinivasan's work there is no stabilising trend. This may be due to the fact that in the present model a closed loop for feed water flow path is used while for the one in [7] an open loop path for feed water is assumed. Increase in  $m_{di}$  is more rapid when compared with the increase in  $m_{wo}$  Fig. 13 (e and f). This fact leads to a decrease in drum water volume initially. But after 22 seconds  $m_{wo}$  becomes greater than  $m_{di}$  leading to an increase in the drum water volume. This increasing drum water volume phenomenon is called swelling in the drum. Gradually as time elapses swelling decreases. After the initial increase in  $m_{wo}$  and  $m_{di}$  both decrease due to increased friction losses. Our results in this case do not entirely match with the results in [7] and [1]. Curve cc of Fig. 12 represents the trend of the high pressure heater II out-let feed water flow rate. H.P. heater II out-let flow rate is assumed to be the same as that of the inlet flow rate into the drum. Here we notice an initial decrease in  $W_{HH2}$ . As we have seen earlier  $P_{dr}$  increases

initially. Both of the above facts lead to an initial rapid increase in  $m_{di}$ . In the cases in [7] and [1]  $w_{HH2}$  remains constant during the test due to its open loop nature for feed water flow path. But in the present case  $w_{HH2}$  is also a variable due to the closed loop nature of the feed water flow path. These may be the reasons for the mismatch.

Steam leaving the H.P. turbine into the reheatere,  $w_{CR}$  is represented by the curve dd of Fig. 12. Pressure and temperature of the H.P. turbine,  $P_{CR}$  and  $T_{CR}$  are showing an increasing trend initially as shown by curves k and l. This is quite expected due to the increase in  $w_1$ . Equation (3.85) shows that when the density of the steam inside the Triflex reheatere (which also receives heat from elevated flue gas temperature) increases, there is a decreasing tendency in  $w_{R01}$ . This is shown by the curve aa of Fig. 12. But after five seconds  $w_{R01}$  increases and then gradually decreases and stabilises. Due to the increased heat inflow rate into the reheatere metal the pressure and temperature inside the reheatere increase as explained by the curves for  $P_{R01}$  and  $T_{RS1}$ . Trends for  $P_{R01}$  and  $T_{RS1}$  are given by the curves m of Fig. 13 and bb of Fig. 12 respectively. The steam which flows out of the first and second stages of the M.P. turbine,  $w_{MP1}$  and  $w_{MP2}$ , shows a similar trend as that of  $w_{R01}$  and is shown in Fig. 12(ce, gg). Those are expected trends because of the behaviour of  $w_{R01}$ .

gradually decrease and then stabilise. Due to the behaviour of  $P_{dr}$  steam flow out of the drum also increases initially and then decreases. This fact leads to an initial increase in primary superheater pressure  $P_{s1}$  and secondary superheater pressure  $P_{s2}$ . Similar trend is noted in the case of respective temperatures  $T_{s1}$  and  $T_{s2}$ . In both the superheaters pressures and temperatures stabilise after some time. Due to the rapid increase in  $P_{dr}$  downcomer inlet flow,  $m_{di}$  increases initially. After the initial increase  $m_{di}$  decreases due to two reasons; one is due to the gradual decrease in  $P_{dr}$  and the other is due to the increased friction losses. Due to the increase in  $m_{di}$  waterwall outflow rate  $m_{wo}$  also increases. After about 20 seconds a little 'swelling' (Fig. 11e and f) is also observed. Due to the momentary increase in  $P_{s2}$  the steam flow rate out of exit reheater  $W_1$  also increases momentarily. When  $P_{s2}$  decrease and stabilise around the steady state value  $W_1$  also shows a similar trend. Curves h and i (Fig. 11) depict the behaviours of  $P_{s2}$  and  $W_1$  respectively.

Steam outflow rate from H.P. turbine  $W_{CR}$  behaves just like that of  $W_1$ . This is quite expected. Steam pressure  $P_{CR}$  leaving the H.P. turbine also shows and expected increasing tendency initially. After reaching the maximum values  $P_{CR}$  and  $T_{CR}$  decrease and stabilise around steady state values. Curves cc and dd of Fig. 10 depict the behaviour of  $T_{CR}$  and  $P_{CR}$ .

respectively. Due to the increased inflow rate into the Triflex reheat, density inside the Triflex reheat increases initially. This leads to an initial set back in the flow rate out of the Triflex reheat,  $W_{R01}$  (Eqn. 3.83). This set back is propagated to the flow rates in all the components after the Triflex reheat. After the initial set back in  $W_{R01}$  it increases and then gradually decreases to stabilise around a steady state value as shown by curve bb of Fig. 10. Curves aa and jj of Fig. 10 and j of Fig. 11 show a similar trend as that of  $W_{R01}$  for  $W_{R02}$ ,  $W_{MPL}$  and  $W_{HH2}$  respectively. Fuel flow rate is assumed to be constant throughout the test. We have noticed a net increase in all of the flow rates. Due to the increased flow rate more heat transfer from the metal wall to the working fluid takes place. This increased heat transfer rate leads to the decrease in the metal wall temperature. As the metal wall temperature decreases the heat transfer rate from the metal walls to the preheater I air and economiser water decrease. This results in a decrease of temperatures of air preheater I air and economiser water as shown by curves l and k of Fig. 11. Following the same argument as in the previous article the behaviours of  $Q_{HLMW}$  and  $Q_{LIMW}$  can be explained. They are represented by curves ff and gg of Fig. 11 respectively.

### 5.2.3 20 percent step increase in throttle valve area, A

The various responses obtained for the area change is

plotted in Fig. 9. Throttle valve area A is given a 20 per cent step increase to conduct the test. This causes a sharp increase in steam flow rate,  $W_1$ . Due to the sudden release of steam out of the exit superheater causes a drop in exit superheater pressure  $P_{s2}$  (Fig. 9d). The behaviour of  $W_1$  and  $P_{s2}$  are as shown by curves c and d of Fig. 9. As time elapses both  $W_1$  and  $P_{s2}$  stabilise. As the pressures in the superheaters decrease the steam flow rate  $m_{ri}$  out of the drum increases initially. But as time elapses  $m_{ri}$  shows a stabilising tendency. The rapid decrease in temperature of the exit reheat steam temperature  $T_{s2}$  is due to the assumption made in the equation (3.61) that is due to its dependence on  $h_{s2}$  and density in the exit reheat. Due to the nearness of the throttle valve to the secondary superheater, when a step change in area is given exit reheat steam properties are more affected than that of Triflex reheat steam properties (Fig. 9 b and c).  $T_{s2}$  fluctuates much more than that of  $T_{s1}$ . Due to the pressure decrease in Triflex reheat  $T_{s1}$  also decreases. But  $T_{s1}$  stabilises more quickly than  $T_{s2}$ . As  $W_1$  increases heat flow rate into the waterwall does not increase because fuel flow rate is kept constant during the test. This leads to a decrease in  $P_{dr}$ . Latent heat of evaporation increases with decrease in pressure  $P_{dr}$ . This will again decrease  $P_{dr}$  due to the lesser amount of steam generation. This decrease in  $P_{dr}$

propagates down stream to cause a decrease in  $P_{S1}$  and  $P_{S2}$  (Fig. 9d). Triflex reheater steam temperature  $T_{RS1}$  decreases initially and then increases gradually to stabilise. Since  $W_1$  increases the flow rate through the Triflex reheat  $W_{R01}$  and the flow rate through the exit reheat  $W_{R02}$  increases (Fig. 9g). But the heat inflow rate into the metal wall does not increase. As  $W_{R01}$  increases heat inflow rate into the steam from the metal wall increases. Due to this there is a decrease in reheat metal wall temperature. This fact leads to the decrease in  $T_{RS1}$  initially (Fig. 9f). Because  $W_1$  increases the flow rate through the H.P. heater No. II,  $W_{HH2}$ , shows an expected increase initially (Fig. 9h).  $W_{HH2}$  also stabilises as time elapses. Fig. 9i shows the behaviour of L.P. heater No. I metal to water heat transfer rate,  $Q_{LIMW}$ . Due to the increase in flow rate through the L.P. heaters  $Q_{LIMW}$  also increases. After the initial increase like all other parameters  $Q_{LIMW}$  also shows a stabilising trend. We have seen that the flow rate increases in most of the components leading to the decrease in metal wall temperatures of various components. The same argument holds good in the case of air preheaters also. Temperature of the air leaving preheater I,  $T_{PLA}$  decreases initially and then gradually increases to stabilise around a steady state value.

### 5.3 Comments

The stabilising tendency of the parameters under consideration can be more clearly observed and explained when the entire system in the closed loop model for the feed water is considered as in the present case. Such trends were either only partially observable or absent from the incomplete models studied in subsystems II and III separately.

## CHAPTER 6

### CONCLUSIONS AND SUGGESTIONS FOR FUTURE WORK

#### 6.1 Conclusions

A mathematical model for a 110 MW thermal unit at Panki Thermal Power Station has been developed. For the sake of simplicity the entire thermal unit has been divided into three major subsystems.

- i) Subsystem I consists of economiser, air preheaters, fuel feeding system including pulverisers and forced draft fan, and the furnace including the burners
- ii) Subsystem II consists of boiler drum, downcomer, water-walls, and primary and secondary superheaters.
- iii) Subsystem III consists of high pressure, medium pressure and low pressure turbines, steam regulating system, throttle valve, reheaters condenser and feed water heaters.

Subsystem I has been modelled in this thesis whereas the models for subsystem II and III have been referred from [7] and [9]. The three systems have then been combined including a closed loop feed water path. Thus a complete model for the entire thermal side of the power plant has been obtained.

The entire mathematical model has forty ordinary non-linear differential equations and one hundred and seventeen algebraic equations involving non-linear relationships between the parameters of the system. Some of the important input parameters whose variations studied are fuel flow rate, feed water flow rate, and throttle valve opening area. The effect of these variations on the transient behaviour of some important output parameters such as drum pressure, superheater pressures, steam flow rate through throttle valve, steam flow rate through the turbine stages etc. have been obtained.

In this study a stabilising tendency of most of the system parameters is observed. This can be explained when the entire system in the closed loop model for the feed water is considered. Such trends were either only partially observable or absent from the incomplete models studied previously in the subsystems II and III separately. From the plots, the system parameter variations on the boiler and turbine side can be simultaneously studied.

### 6.2 Suggestion for Future Work

The above study was carried out under open loop control mode and the automatic control schemes for variations in power level and turbine speed have not been taken into account. The control schemes and hierarchy should also be considered as a next step towards completing the model. The model on the

73(a)

electrical generation side which is coupled to the turbine, should also be incorporated to study the entire system.

Obviously this is going to be more exhaustive and difficult.

An attempt was made in March, 1978 to procure transient data by conducting 10 MW and 20 MW step power drops at Panki Thermal Power Station. In these tests open loop control mode was used to simulate our model. Unfortunately due to inadequate and somewhat crude instrumentation (which may be sufficient for the effective operation of the plant) only qualitative trends for some of the parameters could be obtained. Some of these trends match qualitatively with our theoretical results. It is hoped that the more accurate study could be done by conducting actual tests on the plant with somewhat more sophisticated instrumentation.

The integrated model for the entire unit including thermal, systems generation, distribution and control can be simulated on a hybrid facility. This can be used for generating theoretical data for the parameters of choice which can be used for future design. The facility can also be used as a trainer for the technical staff directly responsible for running the power station.

## APPENDIX I

The important specifications of the 110 MW Panki Thermal Power Plant

Manufacturers	BHEL, INDIA
Generating Capacity	110 MW
Steam Flow rate	375 Tons/hr
Live Steam temperature	540°C
Pressure at the final superheater outlet	139 Kg/cm <sup>2</sup>
Fuel	Pulverised Coal
Calorific Value of the Fuel	4727 K Cals/Kg
Ash content of the fuel	32 percent by weight

## PLANT DATA

Heating surface area of economiser	2880 m <sup>2</sup>
Heating surface area of air preheater one and two together	18720 m <sup>2</sup>
Metal weight of economiser	62570.15 Kgs.
Metal weight of air preheater one and two together	78620.36 Kgs
Water content in the economiser	22 m <sup>3</sup>

## MODEL CONSTANTS

C <sub>P1GM</sub>	=	0.8099
C <sub>P1MA</sub>	=	0.8022
C <sub>P1A</sub>	=	0.25
C <sub>P1M</sub>	=	0.164
C <sub>P2GM</sub>	=	1.055
C <sub>P2MA</sub>	=	1.1627
C <sub>P2A</sub>	=	0.25
C <sub>P2M</sub>	=	0.164
COEFF	=	1.063x10 <sup>-8</sup>
C <sub>EMW</sub>	=	2361.36
C <sub>HMS</sub>	=	0.6125
C <sub>CO2</sub>	=	1.01
C <sub>N</sub>	=	0.16608
C <sub>H<sub>2</sub>O</sub>	=	1.0
C <sub>throttle</sub>	=	0.878
CONST	=	0.5899
C	=	0.04919
C <sub>S1</sub>	=	0.164
C <sub>S2</sub>	=	0.164
C <sub>k1</sub>	=	96.5
C <sub>k2</sub>	=	45000.0
C <sub>WM</sub>	=	0.164
C <sub>F</sub>	=	4727

Some of the model constants are available in [7] and [9]

## REFERENCES

1. K.L. Chien, E.I. Ergin, C. Ling and A. Lee, 'Dynamic Simulation of Boiler', Trans. ASME, Vol. 80, pp. 1809-1819, (1958).
2. E.K. Eckert, 'Heat and Mass transfer', McGraw-Hill, (1959).
3. H.N. Kwan and J.H. Anderson, 'A Mathematical Model of a 200 MW Boiler', Int. J. Control, Vol. 12, No.6, pp 977-998, (1970).
4. M.A. El-Ramly, G.R. Lovejoy, J.A. Makuch, 'Mathematical Model for the Air-Gas Path and Control System of a Balanced Draft Boiler', Third Power Plant Dynamics, Control and Testing Symposium, The University of Tennessee College of Engineering, September 7-9, (1977).
5. Robert Siegel, John R. Howell, 'Thermal Radiation Heat Transfer', McGraw-Hill, (1972).
6. H.G. Kwanty, J.P. McDonald and J.H. Spare, 'A nonlinear model for Reheat Boiler-Turbine-Generator Systems', Part II Development.
7. C.N. Srinivasan, M.Tech. Thesis, Department of Mechanical Engineering, I.I.T. Kanpur (1977).
8. W.J. Kearton, 'Steam Turbine Theory and Practice', MLBS. Pitman, London, (1962).
9. Pradeep K. Shah, M.Tech. Thesis, Department of Mechanical Engineering, I.I.T. Kanpur (1978).

10. IBM Interim Report, 'Power System Computer Feasibility Study', Vol. II, Research Division, San Jose, California (1968).
11. A. Ralston and H.S. Wilf, 'Mathematical Methods for Digital Computers', Wiley New York, (1967).
12. BHEL Plant Data Manual for 110 MW Unit, Panki Thermal Power Station, Kanpur.
13. I.L. Kota Instrumentation Manual, Panki Thermal Power Station, Kanpur.
14. Panki Thermal Power Station Plant Drawings, Prepared by Development Consultants Pvt. Ltd.
15. BHEL Maintenance Manual for 110 MW Unit, Panki Thermal Power Station, Kanpur.
16. H. Nicholson, 'Integrated Control of a Non-Linear Boiler Model', Proc. IEE, Vol. 114, No. 10, pp 1569-1576 (1967).
17. J.H. Daniels, M. Enns, R.D. Hottenstine, 'Dynamic Representation of a Large Boiler-Turbine Unit', ASME Paper No. 61-SA-69, ASME Summer Annual Meeting (1961).

NOMENCLATURE

$A_d$	:	Cross sectional area of downcomer, ( $m^2$ )
$\alpha_g$	:	Absorptivity of <del>fuel</del> gas
$A_T$	:	Flow area available for a partially opened valve ( $m^2$ )
$A_w$	:	Cross sectional area of waterwall tubes( $m^2$ )
$A_{WS}$	:	Waterwall effective surface area,( $m^2$ )
$A_1, A_2$	:	Equivalent areas for I and II reheater tubes respectively ( $m^2$ )
		Constants used in flow, pressure relations for governing stage
CCA	:	Constants used in the equations for flow Area of the throttle valve, ( $m^2$ ) )
$c_g$	:	Specific heat of <del>fuel</del> gases, (kcals/kg)
$c_N$	:	Constant for pipe flow from drum to superheater
$c_F$	:	Calorific value of pulverised coal,(kcals/kg)
$c_{PS}, c_{HS}$	:	Coefficient of heat transfer from super heater metal to steam in primary and secondary superheaters.
$c_{HMS}$	:	Coefficient of heat transfer between primary superheater metal and furnace
$c_{HMSS}$	:	Coefficient of heat transfer between secondary superheater metal and furnace.
$c_{WM}, c_{S1}, c_{S2}$	:	Specific heat of waterwall and <sup>primary</sup> secondary superheater metals respectively (kcals/kg °C)
CONST	:	Coefficient of heat transfer between waterwall metal and two phase mixture
$c_1 \dots c_{19}$	:	Model constants

$C_{P1GM}$	:	
$C_{P2GM}$	:	Coefficients of heat transfer between flue gas to metal of air preheater I, air preheater II and economiser
$C_{EGM}$	:	
$C_{P1M}, C_{P2M}$	:	Specific heats of airpreheater I and II and economiser (Kcals/Kg °C)
$C_{EM}$	:	
$C_{P1A}, C_{P2A}$	:	Specific heats of Air inside airpreheater I and II (Kcals/Kg °C)
$C_{EW}$	:	Specific heats of water inside the economisor (Kcals/Kg °C)
$C_{P1MA}$	:	Coefficientsheat transfer between air-preheater I and II and air
$C_{P2AMA}$	:	
$C_{EMW}$	:	Coefficientsheat transfer between economiser metal and water
$C_{TM1}$	:	Specific heat of the metal in reharter I
$C_{TM2}$	:	and II (Kcals/Kg °C)
$C_{RMS1}$	:	Constants used in the model
$C_{RMS2}$	:	
$C_{cw}$	:	Constant
$C_{HMW1}, C_{HMW2}$	:	Constants used in the heat flow equations in the four L.P. heaters respectively
$C_{HMW3}, C_{HMW3}$	:	
$C_{HMW5}, C_{HMW6}$	:	Constants used in the H.P heater model
$D_d, D_w$	:	Diameter of Downcomer and waterwall tubes respectively.(m)
$\Delta\epsilon$	:	Correction factor used in emissivity equation
$\epsilon_G, \epsilon_{CO_2}$	:	Emissivity of <del>fuel</del> gas, carbon dioxide and water vapour in the combustion chamber respectively
$\epsilon_{H_2O}$	:	
$f$	:	Vector function

$f_d, f_w,$	:	Friction factors in the downcomer, water-wall, Triflex and exit reheatere respectively
$F_{R1}, F_{R2}$	:	
$g$	:	Acceleration due to gravity ( $m/sec^2$ )
$h_{eo}, h_{ds}$	:	Enthalpy of feedwater, attemperation spray, water in the drum, steam in the drum, steam leaving the drum, water at downcomer inlet, steam at the outlet of water walls, steam at the exit of throttle valves and steam at the exit of governing stage. (Kcals./Kg)
$h_{drw} (=h_{wow}),$	:	
$h_{drs} (=h_{wos}),$	:	
$H_{SS}, H_{HP}$	:	
$h_{ri}, h_{di},$	:	Enthalpies of steam leaving drum, water at downcomer inlet, steam in primary super-heater, steam in secondary super-heater, steam at steady state operating temperature in super-heaters (Kcals./Kg)
$h_{wo}, h_{sl},$	:	
$h_{s2}, h_{st1},$	:	
$h_{st2}$	:	
$H_{CR}, H_{CRA},$	:	Enthalpies of reheatere steam (ideal and actual), steam at the exit of triflex and exit reheatere, attemperation water, ideal enthalpy of steam at the exit of each M.P. turbine.
$H_{R01}, H_{R02},$	:	
$H_{AMP}, H_{MP1},$	:	
$H_{MP2}, H_{MP3},$	:	
$H_{MPO}$	:	
$H_{MP1A}, H_{MP2A}$	:	Actual enthalpy of steam at the exit of each M.P. turbine (Kcals./Kg)
$H_{MP3A}, H_{MPOA}$	:	
$H_{LPO}, H_{LPOA}$	:	Ideal and actual enthalpy at the exit of L.P. turbine (Kcals./Kg)
$H_{LH10}, H_{LH20}$	:	Enthalpy of water at the exit of four L.P. heaters and at the exit of two H.P. heaters. (Kcals./Kg)
$H_{LH30}, H_{LH40}$	:	
$H_{HH10}, H_{HH20}$	:	
$J$	:	Conversion factor for converting work to heat energy
$k_1, k_2$	:	Callender's empirical constants.

$K_p, K_1, K_2$	Constants used in the model
$K_3, K_4, K_5$	
$L_{db}, L_{df},$	Vertical length of downcomer, flow length of downcomer, flow length of water wall (m)
$L_{wf}$	
$L_1, L_2$	Equivalent length of tubes in the triflex and exit reheater respectively (m)
$M_1, M_2, \dots$	Mass of primary sup.heater metal, secondary sup.heater metal reheaters one and two, Air preheaters one and two and economiser metal. (Kg.)
$m_{eo}, m_{ri},$	Mass flow rate of feed water, steam going out of drum, water at down comer inlet,
$m_{di}, m_{do}, m_{wo},$	water at downcomer outlet, two phase mixture at waterwall outlet, effective steam mass at reheaters one and two respectively. (Kg/sec.)
$M_{P1A}, M_{P2A},$	Resident mass of air in airpreheaters one and two and water in the economiser (Kg.)
$M_{EW}$	
$P_{SS}$	Steam pressure before throttle valves (Kg/m <sup>2</sup> )
$P_{dr}, P_{do},$	Pressure at drum, downcomer outlet, pressure in the primary and secondary
$P_{s1}, P_{s2}$	sup.heaters respectively (Kg/m <sup>2</sup> )
$P_{THI} (I=1,2,3)$	Nozzle ring pressure in the three streams (Kg/m <sup>2</sup> )
$P_{HP}$	Steam pressure at the exit of curtis stage (Kg/m <sup>2</sup> )
$P_{CR}$	Cold reheat steam pressure (Kg/m <sup>2</sup> )
$P_{ROL}, P_{RL2},$	Steam pressure at the exit of triflex and exit reheater. Inlet steam pressure to
$P_{MPI}, P_{MPL},$	M.P. turbine, pressure at the exit of
$P_{MP2}, P_{MP3},$	4 M.P. turbines and condenser pressure respectively. (Kg/m <sup>2</sup> )
$P_{MPO}, P_{LPO}$	

$P_{OW_2}, P_{OW_3},$	:	Power produced by each of the M.P. turbines
$P_{OW_4}, P_{OW_5}$	:	respectively (MW)
$P_{OW_6}$	:	Power produced by L.P. turbine (MW)
$Q_{S1}, Q_{S2}, Q_w,$	:	Heat flow rate to steam in the primary and secondary superheater, two-phase mixture in waterwalls, primary sup. heater metal from flue gases, secondary sup. heater metal and waterwall metal from gases respectively (Kcals/sec.)
$Q_{SM1}, Q_{SM2},$		
$Q_{GW}$		
$q_{s1}, q_{s2}$	:	Net heat content of steam in the primary and secondary superheater respectively. (Kcals.)
$Q_{RG1}, Q_{RG2},$	:	Heat flow to triflex and exit reheat metal walls, heat flow to triflex and exit reheat steam and heat flow to the condenser cooling water. (Kcals/sec.)
$Q_{RS1}, Q_{RS2},$		
$Q_{MW}$		
$Q_{LH1MW},$	:	Heat added to feed water in the four L.P. heaters and two H.P. heaters (Kcals/sec.)
$Q_{LH2MW},$		
$Q_{LH3MW},$		
$Q_{LH4MW},$		
$Q_{HH1MW},$		
$Q_{HH2MW}$		
$Q_{P1GM}, Q_{P2GM}$	:	Heat flow to metal of Air preheater I and II and economiser metal from gas. (Kcals/sec.)
$Q_{EGM}$		
$Q_{P1MA}, Q_{P2MA}$	:	Heat flow to the air in Air preheater I and II from the metal and heat flow to the economiser water from the economiser metal (Kcals/sec.)
$Q_{EMW}$		
$\sigma$	:	Stefan Boltzman constant used in radiative heat transfer calculations.

$T_0, T_2, T_3, T_4,$	:	Time constants of H.P. turbine, four M.P. turbines, L.P. turbine and triflex reheater and Exit reheat
$T_{CL}$	:	Time constant in the sup.heater
$T_{dr}, T_{S1}, T_{S2},$ $T_{SM1}, T_{SM2},$ $T_{gw}, T_{ST1}, T_{ST2}$	:	Saturation temp.in the drum, Temperature of steam in the primary and secondary sup.heater, metal of primary and secondary sup.heater, flue gas in the furnace, steady state operating temp. of steam in the primary and secondary sup.heaters ( $^{\circ}\text{C}$ )
$T_{R1}, T_{R2},$ $T_{H1}, T_{H2}$	:	Constants used in the model
$T_{SS}, T_{HP}, T_{CR}$	:	Temp. of steam before throttle valve, steam at the exit of curtis stage and cold reheat steam. ( $^{\circ}\text{C}$ )
$T_{RM1}, T_{RM2}, T_{RS1},$ $T_{RS2}, T_{MP1}, T_{MP1},$ $T_{MP2}, T_{MP3}, T_{MPO}$	:	Temperature of tube metal of triflex and exit reheater. Steam in triflex and exit reheat, steam at inlet to M.P. turbine, steam at the exit of four M.P. turbines respectively. ( $^{\circ}\text{C}$ )
$T_{LFO}, T_{CM}, T_{CW},$ $T_{HM1}, T_{HM2}, T_{HM3},$ $T_{HM4}, T_{HM5}, T_{HM6}$	:	Temperature of condenser tube metal and cooling water, tube metal of four L.P. heaters and two H.P. heaters. ( $^{\circ}\text{C}$ )
$T_{HW1}, T_{HW2}, T_{HW3},$ $T_{HW4}, T_{HW5}, T_{HW6}$	:	Temp. feed water in four L.P. heaters and two H.P. heaters ( $^{\circ}\text{C}$ )
$T_{P1M}, T_{P1G}, T_{PLA},$ $T_{P2M}, T_{P2G}, T_{P2A}$ $T_{EM}, T_{EG}, T_{EW}$	:	Temperature of Air preheater I metal, flue gas and air, Air preheater II metal, flue gas and air, Economiser metal, flue gas and water. ( $^{\circ}\text{C}$ )

$V_d, V_w, V_{dr}, V_{sl},$	:	Volume downcomer tubes, water wall tubes, drum, primary and secondary superheater, water wall tube metal, drum water, steam in the drum respectively. ( $m^3$ )
$V_{R1}, V_{R2}$	:	Effective volume of steam in Trifler and exit reheaters. ( $m^3$ )
$W_1, W_o$	:	Mass flow rate of steam at secondary and primary sup. heater outlet. ( $Kg/sec$ )
$W_F, W_{AF} (=W_A), W_G$	:	Fuel flow rate and Air flow rate and flue gas flow rate ( $Kg/sec.$ )
$W_{ASH}$	:	Ash content of pulverised coal. (%)
$W_{DS1}, W_{DS2}$	:	Mass flow rate of attemperation spray I and II ( $Kg/sec.$ )
$(W_T)_V, (W_T)_N,$	:	Flow rate, through the throttle valve, through the nozzle ring, flow rate of cold reheat steam and rated flow of the turbine. ( $Kg/sec.$ )
$W_{CR}, W_R, W_N$	:	
$W_L$	:	Ratio of $W_N$ and $W_R$
$W_{RI2}, W_{RO1},$	:	Flow rate of steam air exit reheater inlet, at the exit of trifler and exit reheater, attemperation added to steam before M.P. turbine inlet, steam entering M.P. turbine. ( $Kg/sec.$ )
$W_{RO2}, W_{ATMP},$	:	
$W_{MPI}$	:	
$W_{MP1}, W_{MP2},$	:	Steam flow at the exit of the four M.P. turbines respectively. Flow to condenser, quantity of cooling
$W_{MP3}, W_{MPO},$	:	water in the condenser. ( $Kg/sec.$ )
$W_{LPO}, W_{CW}$	:	
$W_{L1}, W_{L2},$	:	Quantity of feed water passing through the four L.P. heaters and two H.P. heaters. ( $Kg/sec.$ )
$W_{LH3}, W_{LH4},$	:	
$W_{HH1}, W_{HH2}$	:	

$\rho_{drw}$ ( $= \rho_{wo}$ ),	:	Density of water in the drum, steam in the drum, water at downcomer inlet and outlet two phase mixture at water-wall outlet, steam in the primary and secondary sup. heaters, waterwall metal, steam at steady state operating temperature in sup. heater I and II and air from the atmosphere respectively. ( $\text{Kg/m}^3$ )
$\rho_{drs}$ ( $= \rho_{wos}$ ),	:	
$\rho_{di}, \rho_{do}, \rho_{wo},$	:	
$\rho_{s1}, \rho_{s2}, \rho_{WM},$	:	
$\rho_{ST1}, \rho_{S2}, \rho_{air}$	:	
$\rho_{SS}, \rho_{THI}, \rho_{HP},$	:	Density of steam before throttle valve
$\rho_{R1}, \rho_{R2}, \rho_{MP2},$	:	steam in the nozzle ring, steam at
$\rho_{MP2}, \rho_{MP3}$	:	the exit of governing stage, steam in
		the triflex and exit reheater, steam
		in the three M.P. turbines respectively ( $\text{Kg/m}^3$ )
$\eta, \eta_{HP}, \eta_{MP},$	:	Burning efficiency for combustion,
$\eta_{LF}, \eta_F, \eta_{F1},$	:	efficiencies of H.P., M.P. and L.P.
$\eta_{F2}, \eta_{F3},$	:	turbines, efficiency correction
$\eta_{F4}, \eta_{F5}$	:	factor, for H.P. turbine, for each of
		the four M.P. turbines and correction
		factor for L.P. turbine
$\eta_{HPA}, \eta_{MP1},$	:	Actual efficiency of H.P. turbine,
$\eta_{MP2}, \eta_{MP3},$	:	Actual efficiencies of each of the
$\eta_{MP4}, \eta_{LPA}$	:	four M.P. turbines and actual
		efficiency of L.P. turbine.

A 59255

Date Slip A 59255

This book is to be returned on the date last stamped.

CD 6.72.9

ME-1979-M-NON-DYN